J. Nonlinear Sci. Vol 2: pp. 135–182 (1992)

Journal of Nonlinear Science

The Transition from Bursting to Continuous Spiking in Excitable Membrane Models

D. Terman[1]

Department of Mathematics, Ohio State University, Columbus, OH 43210 and Mathematics Research Branch, NIDDK, Bldg. 31, Rm. 4B-54, National Institute of Health, Bethesda, MD 20892, USA

Recieved July 16, 1991; accepted for publication November 22, 1992
Communicated by Stephen Wiggins

Summary. Mathematical models for excitable membranes may exhibit bursting solutions, and, for different values of the parameters, the bursting solutions give way to continuous spiking. Numerical results have demonstrated that during the transition from bursting to continuous spiking, the system of equations may give rise to very complicated dynamics. The mathematical mechanism responsible for this dynamics is described. We prove that during the transition from bursting to continuous spiking the system must undergo a large number of bifurcations. After each bifurcation the system is increasingly chaotic in the sense that the maximal invariant set of a certain two-dimensional map is topologically equivalent to the shift on a larger set of symbols. The number of symbols is related to the Fibonacci numbers.

Key words. bursting oscillations, excitable membranes, Fibonacci dynamics.

I. Introduction

In a recent paper [17] we considered certain systems of differential equations which model excitable membranes. These include models for electrical activity in pancreatic β-cells; see [3], [4], and [16]. We demonstrated that the equations must give rise to sustained oscillations of the burst type and, for larger values of a parameter, the bursting gives way to continuous spiking. In Figure 1A we see an example of a bursting solution. It is characterized as a periodic solution whose behavior alternates between near steady-state behavior (the passive phase) and trains of spike-like oscillations (the active phase). The bursting solutions correspond, for example, to the pancreatic β-cell's response to the presence of glucose [2], [10], and this activity is correlated with their release of insulin [15]. Continuous spiking corresponds to stable periodic solutions which always oscillate in the active phase; it is analogous to the sustained excitation seen physiologically in the presence of high concentration of agonist. An example of such a solution is shown in Figure 1B. Each solution shown in Figure 1 is a solution of the system (A.1) that is described in the Appendix.

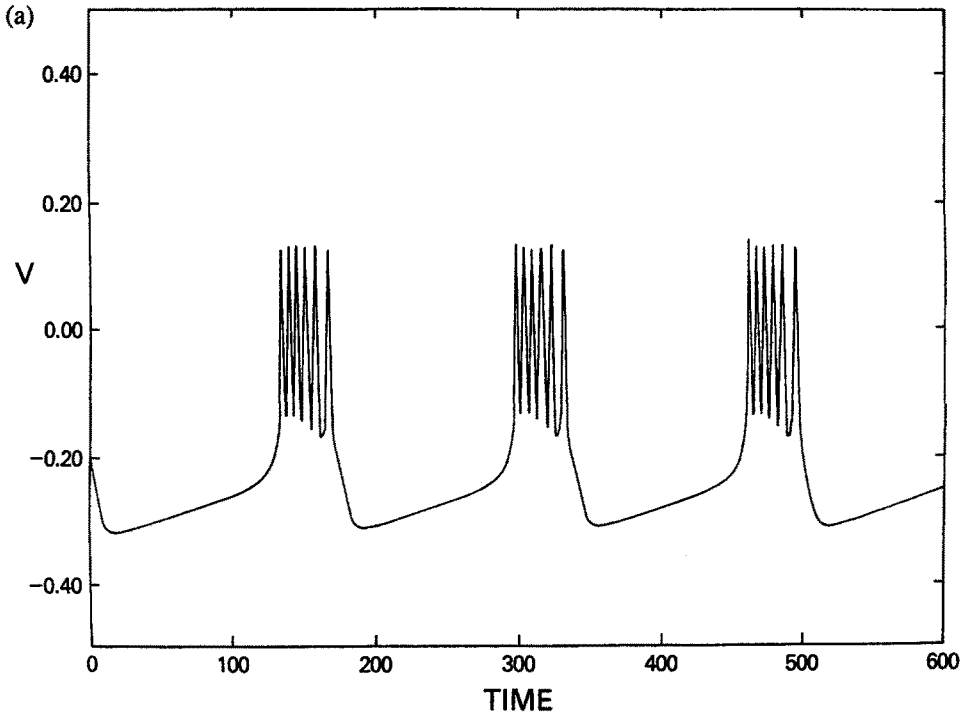
(a)
0.40
0.20
V
0.00
−0.20
−0.40
0
100
200
300
400
500
600
TIME

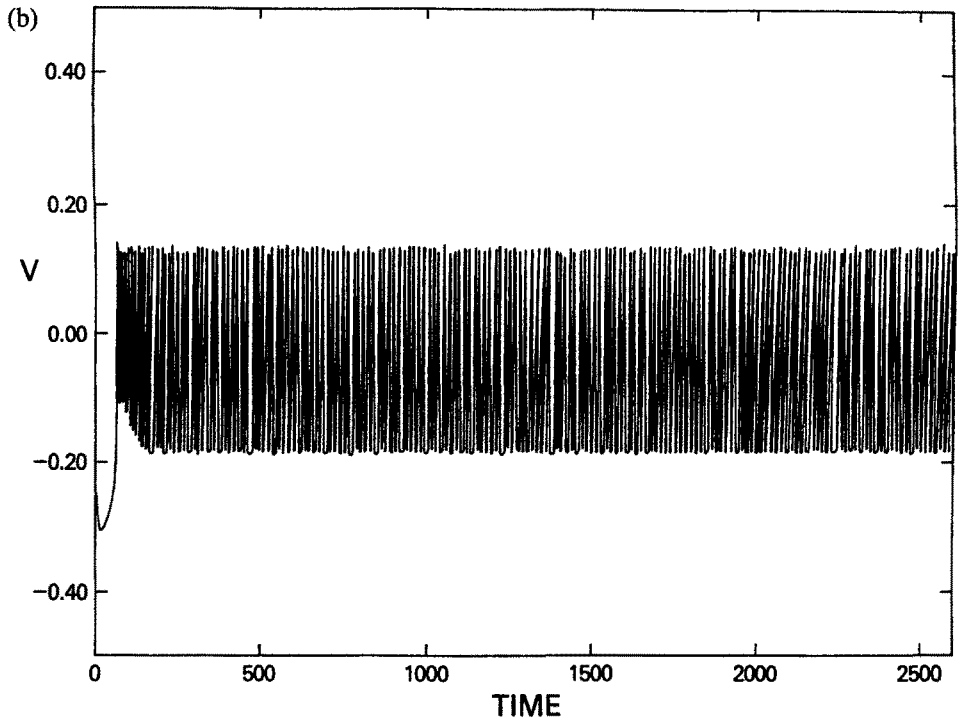
(b)
0.40
0.20
V
0.00
−0.20
−0.40
0
500
1000
1500
2000
2500
TIME

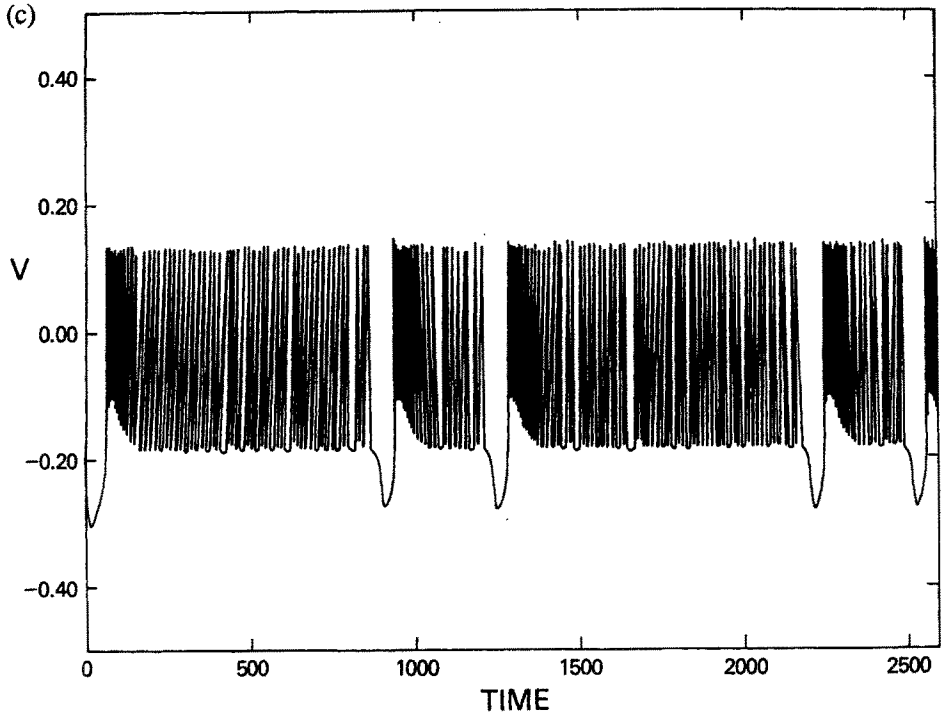

Fig. 1. Solutions of (A.1) with $\epsilon = .002$, and (A) $k = -.23$, (B) $k = -.13$, and (C) $k = -.1306$. The solution in (A) is bursting, the solution in (B) corresponds to continuous spiking, and the solution in (C) demonstrates the chaotic transition from bursting to continuous spiking.

In this paper we study how solutions of the equations make the transition from bursting to continuous spiking as parameters in the equations are varied. Numerical results [5] have demonstrated that during this transition the system gives rise to very complicated dynamics. Such a solution is shown in Figure 1C. This solution is "burst-like" in the sense that its behavior alternates between near steady-state behavior and spike-like oscillations. However, there is no fixed period for each burst; the amount of time each burst spends in its active phase is very irregular. Note that there may be very long active phases followed by relatively short active phases.

Our goal is to describe the mathematical mechanisms responsible for the irregular, or chaotic, solution illustrated in Figure 1C. We prove that for the class of models considered in [17], chaotic dynamics must arise during the transition from bursting to continuous spiking. The dynamics is characterized in terms of a two-dimensional map, π, which is defined in Section 3. We say that the system gives rise to chaotic dynamics if the maximal invariant set of π is topologically equivalent to the shift map on the set of bi-infinite sequences of j symbols where $j \geq 2$. We prove that during the transition from bursting to continuous spiking, the system must undergo a large number of bifurcations. After each bifurcation, the system gives rise to increasingly more complicated dynamics in the sense that the maximal invariant set of π is topologically

equivalent to the shift on a larger set of symbols. One interesting feature of our results is that the number of symbols is related to the Fibonacci numbers.

The models which we consider are autonomous systems of ordinary differential equations. They are typically expanded versions of the classical Hodgkin-Huxley [9] description of nerve excitation. The first such model for electrical activity in pancreatic β-cells was due to Chay and Keizer [4]. Later, Chay [3] and Sherman, Rinzel, and Keizer [16] introduced three variable models. The three variables represent the membrane potential, the intracellular free calcium concentration, and a potassium state variable.

The systems considered here consist of fast and slow subsystems. If we think of the variables of the slow subsystem as parameters, then the fast subsystem has a branch of stable rest points and a branch of stable periodic solutions. The bursting solution then corresponds to a closed orbit in phase space which, in the passive phase, passes close to the branch of stable rest points. The trains of rapid spikes correspond to the closed orbit passing close to the branch of periodic solutions. See Figure 2. This geometric description of bursting was first proposed by Rinzel [13]. Continuous spiking corresponds to a stable closed orbit in phase space which always lies close to the branch of periodic solutions.

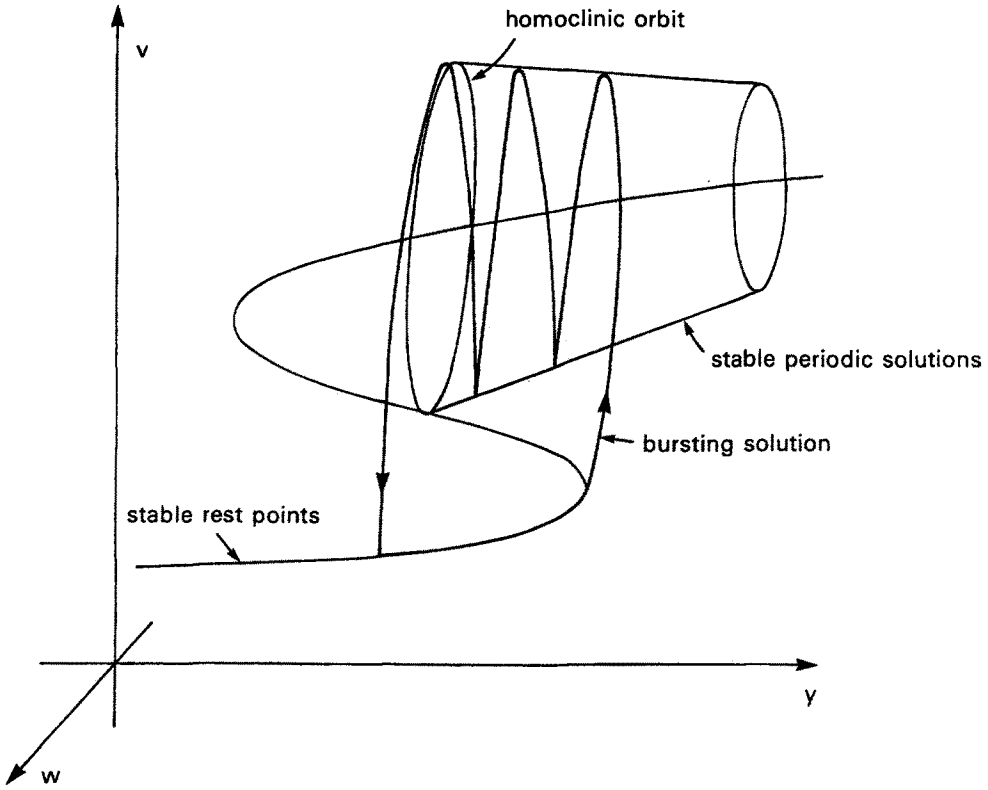

Fig. 2. Geometric model for bursting. The slow variable is y. If y is considered as a parameter, then the fast subsystem (v, w) has a branch of stable rest points and a branch of stable periodic solutions. The bursting solution passes close to the branch of stable rest points in the passive phase and passes close to the branch of stable periodic solutions in the active phase.

An important feature of the systems which we consider is that in the fast subsystem the branch of periodic solutions terminates at a homoclinic orbit. A key step in understanding how the chaotic dynamics emerge is to understand how solutions near this homoclinic orbit behave as parameters in the equations are varied. There have been several papers recently concerning homoclinic bifurcations; see [18], [6] and the references cited there. These results, however, usually assume that the homoclinic point is hyperbolic. For the systems which we consider, the homoclinic orbit exists when a singular perturbation parameter is equal to zero. The homoclinic point is contained in a one-parameter family of fixed points; it is, therefore, degenerate.

In [17] we demonstrated that chaotic dynamics may arise during the process of adding a spike to the active phase of the bursting solutions. The chaotic dynamics described in [17] is, however, quite different from the chaotic dynamics discussed in this paper. The Smale horseshoes constructed in [17] exist for extremely narrow ranges of the parameters. Moreover, most trajectories which, at some time, lie close to the horseshoe will eventually leave a small neighborhood of the horseshoe and never return. The chaotic dynamics considered in this paper, however, has a certain attracting property: Suppose that the map π, which was introduced earlier, gives rise to chaotic dynamics, and Λ is the maximal invariant set of π. Then there exists a small neighborhood of Λ in phase space such that every trajectory lies in this neighborhood infinitely often.

The existence of the chaotic dynamics described here was first recognized by Chay and Rinzel [5]. Their numerical studies suggest that the dynamics can be reduced to a one-variable, logistic-type map. This approach was also taken by Alexander and Cai [1]. The reason that the three-dimensional system can be studied in terms of a one-dimensional map for a large range of parameters is that the system has a strong dissipation property. This will follow from our analysis and is described in further detail in Section 4; see Remark 4G.

An outline of the paper is as follows. Section 2 consists of three parts. In Section 2A, we state precisely what assumptions are required for our systems of equations. In Section 2B, we describe some basic properties of a class of two-dimensional maps. In particular, we define the notion of Fibonacci dynamics. This notion is used in the statement of the main result which is given in Section 2C. In Section 3 we formally define the two-dimensional map π. It will be a first-return map and is defined by solutions of the equations which lie close to the homoclinic orbit of the fast subsystem. Basic properties of π are also proved in Section 3. The proof of the main result is given in Sections 4 and 5, with the more technical aspects of the proof reserved for Section 5.

2. Assumptions, Fibonacci Dynamics, and Results

A. Assumptions

We consider a system of ordinary differential equations of the form

$$\begin{aligned} v' &= f_1(v, w, y), \\ w' &= f_2(v, w, y), \\ y' &= \epsilon g(v, w, y, k). \end{aligned} \tag{2A.1}$$

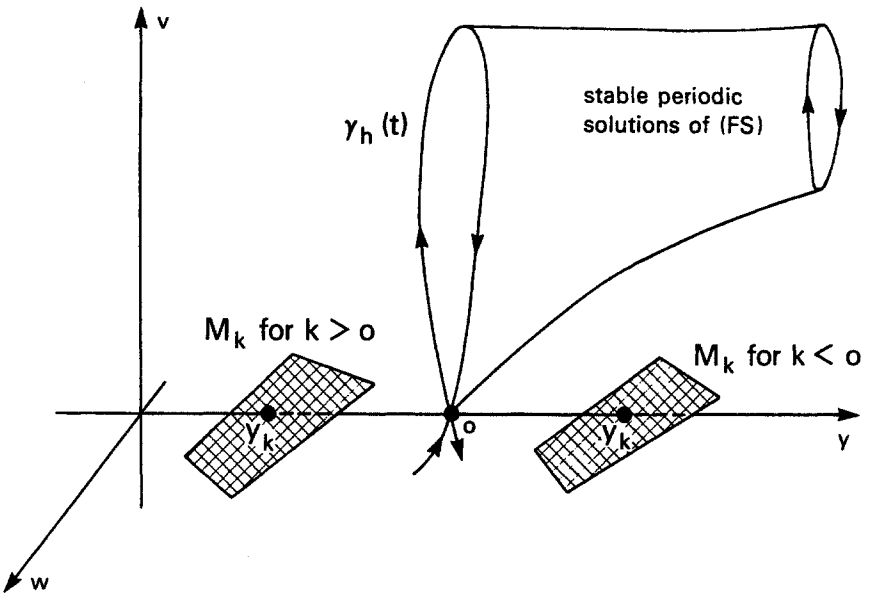

Fig. 3. Objects that appear in assumptions A1–A6. If $\epsilon > 0, |y| < \delta_y$, and $|k| < \delta_k$, then $(0, 0, y_k)$ is a fixed point of (2A.1). If $y = 0$, then (0,0) is a homclinic point of (FS). A branch of stable periodic solutions of (FS) exists for $y > 0$ and terminates at the homoclinic orbit $\gamma_h(t)$.

Here ϵ is a small positive constant, and f_1, f_2, and g are smooth functions. If we let $f(v, w, y) = (f_1, f_2)^T$, then by fast subsystem we mean the equations

$$\begin{pmatrix} v \\ w \end{pmatrix}' = f(v, w, y). \tag{FS}$$

In (FS), the slow variable y is thought of as a parameter.

In [17] we gave conditions on the nonlinear functions in (2A.1) which guarantee that there exist bursting solutions and, for other values of the parameters, continuous spiking. The object of this paper is to demonstrate that chaotic dynamics must arise as the parameters in (2A.1) vary from the range of bursting solutions to the range of spiking. The existence of the chaotic dynamics does not depend, however, on all of the assumptions needed for the existence of bursting solutions or continuous spiking. We first describe only those assumptions needed for the existence of the chaotic dynamics. We shall see that the chaotic dynamics arises from the perturbation of an orbit which is homoclinic to a degenerate fixed point. After we state these assumptions, we shall briefly describe the further assumptions and results in [17] concerning the existence of bursting solutions and continuous spiking.

We now state six assumptions (see Fig. 3). The first four are concerned solely with the fast subsystem (FS). Our first assumption is that there exists a curve of fixed points of (FS) in the (v, w, y) phase space. By a suitable change of variables we may assume that at these fixed points $(v, w) = (0, 0)$.

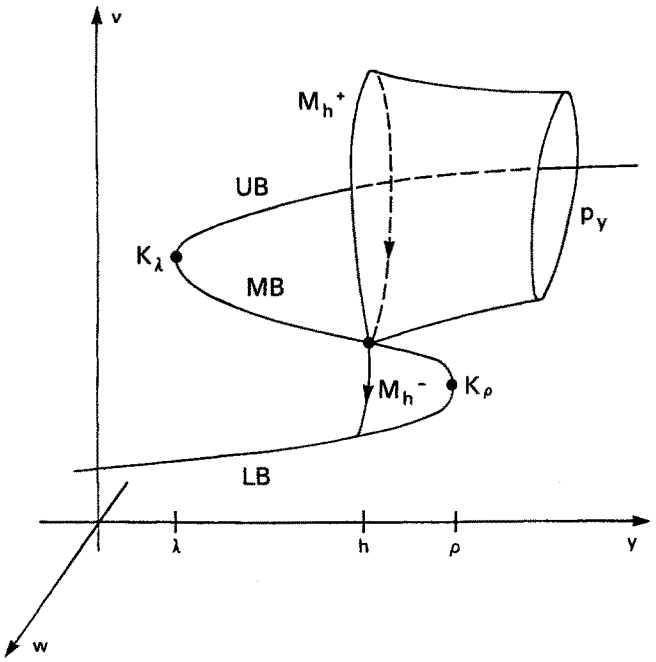

Fig. 4. The phase space of (2A.1). LB, MB, and UB are the branches of rest points of (FS). For $y > h$, there is a branch of stable periodic solutions, which surround UB. This branch terminates at the homoclinic orbit $M_h^+(t)$ as $y \to h$.

A1. There exists a $\delta_y > 0$ such that (0, 0) is a fixed point of (FS) for each $y \in (-\delta_y, \delta_y)$. Each of these fixed points is a saddle.

A2. Suppose that λ_1 and $-\lambda_2$ are, respectively, the positive and negative eigenvalues of (FS) linearized at (0, 0) when $y = 0$. Then $\lambda_1 < \lambda_2$.

Remark. This last condition is satisfied for the models discussed in the introduction.

For $|y| < \delta_y$, let $q_y = (0, 0, y)$ and let $S = \{q_y : |y| < \delta_y\}$. The union of the stable (resp. unstable) manifolds of each q_y forms an invariant, center-stable (resp. center-unstable) manifold which we denote by W^{cs}(resp.W^{cu}).

A3. There exists a solution $\gamma_h(t)$ of (FS) with $y = 0$ which is homoclinic to q_0. This homoclinic orbit arises from the transverse intersection of W^{cs} and W^{cu}.

A4. For each $y \in (0, \delta_y)$ there exists a stable periodic solution of (2A.1). The union of these periodic solutions forms a smooth manifold which terminates at $\gamma_h(t)$ as $y \to 0$.

Our final assumptions are concerned with the slow dynamics.

A5. There exists $\delta_k > 0$ such that if $|k| < \delta_k$, then $g(v, w, y, k) = 0$ if and only if $v = h(w, y, k)$ for some smooth function $h(w, y, k)$. Moreover, $g(v, w, y, k) < 0$ if and only if $v > h(w, y, k)$.

For $|k| < \delta_k$, let $M_k = \{(v, w, y) : v = h(w, y, k)\}$ and $M_k^+ = \{(v, w, y) : v > h(w, y, k)\}$.

A6. If $|k| < \delta_k$, then there exists $y_k \in (-\delta_y, \delta_y)$ such that $M_k \cap S = qy_k$. Moreover, $y_0 = 0$, and, for $|k| < \delta_k$, $dy_k/dk < 0$. Finally, if $k \in (-\delta_k, 0]$, then $\gamma_h(t) \in M_k^+$ for all t.

Remarks. (a) Assumption A6 implies that for each $k \in (-\delta_k, \delta_k)$ and $\epsilon > 0$, (2A.1) has one fixed point in the set where $|y| < \delta_y$. This fixed point is q_{y_k}. Since $dy_k/dk < 0$, this fixed point moves to the "left" as k is increased. Moreover, if $k \in (-\delta_k, 0]$, then $\gamma_h(t)$ lies in the set where $y' < 0$.

(b) Assumptions A2 and A3 imply that there exists a smooth manifold of periodic solutions which terminate at $\gamma_h(t)$. Our assumption that these periodic solutions exist for $y \in (0, \delta_y)$ instead of $y \in (-\delta_y, 0)$ is, of course, arbitrary. However, if in A4 we had assumed that the periodic orbits exist for $y \in (-\delta_y, 0)$ then, for our results, it would have been necessary to assume in A6 that $dy_k/dk > 0$. Chaotic dynamics will not arise from a homoclinic bifurcation if either (a) the periodic solutions exist for $y \in (0, \delta_y)$ and $dy_k/dk > 0$, or (b) the periodic solutions exist for $y \in (-\delta_y, 0)$ and $dy_k/dk < 0$.

We conclude this section by reviewing the results in [17]. Our goal now is to describe the relationship between assumptions A1–A6 and those assumptions required for the existence of bursting solutions and continuous spiking. In order to avoid too many technical details, the discussion here is somewhat informal. The precise assumptions required for the existence of bursting solutions and continuous spiking are listed in the Appendix. In what follows, the reader is referred to Figure 4.

The assumptions required for the existence of bursting solutions and continuous spiking are the following. We first consider the fast subsystem (FS). We assume that the fixed points of (FS) consist of a smooth, S-shaped curve, $\mathcal{S}$, in phase space. That is, there exists $\lambda < \rho$ such that if either $y < \lambda$ or $y > \rho$, then (FS) has precisely one fixed point. If $\lambda < y < \rho$, then (FS) has precisely three fixed points. Each fixed point on the lower branch of $\mathcal{S}$ is assumed to be stable with respect to (FS), while each fixed point on the middle branch of $\mathcal{S}$ is a saddle.

We next consider the set of periodic solutions of (FS). We assume that there exists $h \in (\lambda, \rho)$ such that for each $y > h$, there exists a unique, stable periodic solution of (FS). The union of all of these periodic solutions forms a manifold $\mathcal{P}$ which terminates at an orbit which is homoclinic to the fixed point of (FS) that lies on the middle branch of $\mathcal{S}$ for $y = h$. It is this homoclinic orbit that corresponds to the homoclinic orbit described in Assumption (A3). In Figure 5, we illustrate the phase planes corresponding to (FS) for three different values of the parameter y.

The remaining assumptions needed for bursting solutions and continuous spiking are concerned with the slow equation; this is the last equation in (2A.1). We assume that $M_k \equiv \{(v, w, y) : g(v, w, y, k) = 0\}$ is a smooth, two-dimensional manifold that

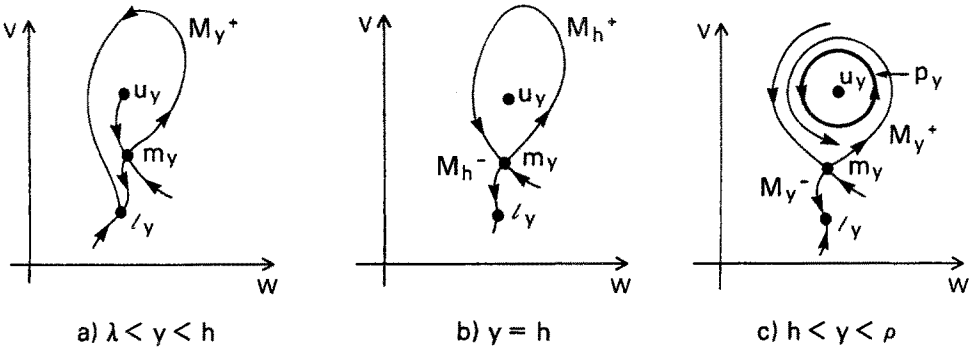

Fig. 5. The phase plane of (FS) for three different values of y. If $\lambda < y < h$, then each trajectory in the unstable manifold of $m_\backslash$ approaches $l_\backslash$ as $t \to \infty$. If $y = h$, then one of these trajectories is the homoclinic orbit. If $h < y < \rho$, then this trajectory approaches the periodic solution, $p_\backslash$, as $t \to \infty$.

intersects $\mathcal{S}$ at precisely one point. We denote this point by p_k and assume that it lies on the middle branch of $\mathcal{S}$ for each k. We assume that $g(v, w, y, k) > 0$ for values of (v, w, y) that lie "below" M_k, and $g(v, w, y, k) < 0$ for values of (v, w, y) that lie "above" M_k. Note that if $\epsilon > 0$, then p_k is a fixed point for the full system (2A.1). Our final assumption is concerned with how the surface M_k changes with respect to the parameter k. We assume that there exists k_h such that if $k < k_h$, then p_k lies "below" the homoclinic point on the middle branch. If $k > k_h$, then p_k lies above the homoclinic point.

In [17], we prove that if $k < k_h$ and ϵ is sufficiently small, then (2A.1) gives rise to a bursting solution. Intuitively, we expect this to be true for the following reason. Suppose that $k < k_h$, ϵ is small, and $\gamma(t)$ is a solution of (2A.1) that begins near the lower branch of $\mathcal{S}$. Because $y' = \epsilon g(v, w, y, k) > 0$ near the lower branch of $\mathcal{S}$, this trajectory will slowly drift to the "right" along the lower branch until it reaches the right knee of $\mathcal{S}$. This corresponds to the passive phase of the bursting solution. The fast dynamics will then force the trajectory close to the manifold $\mathcal{P}$ of stable periodic solutions of (FS). Because $k < k_h$, it follows that $y' < 0$ near $\mathcal{P}$. The trajectory therefore drifts to "left," near $\mathcal{P}$, until it reaches near to the homoclinic point on the middle branch of $\mathcal{S}$. This corresponds to the spiking phase of the bursting solution. In [17], we prove that eventually the fast dynamics forces the trajectory back to near the lower branch. This then completes one period of the bursting solution.

We also prove in [17] that if $k > k_h$ and ϵ is sufficiently small, then (2A.1) gives rise to continuous spiking. This corresponds to a stable peroidic solution of (2A.1) that always lies near the manifold $\mathcal{P}$ of periodic solutions of (FS).

Remark. In order to prove the existence of bursting solutions or continuous spiking, we need to assume that ϵ is sufficiently small. The size of ϵ depends on the choice of k. In particular, we have that $\epsilon \to 0$ as $k \to k_h$. Therefore, there must exist two curves $\epsilon = \epsilon_b(k)$ and $\epsilon = \epsilon_s(k)$ with $\epsilon_b(k_h) = 0 = \epsilon_s(k_h)$ and the following properties: If $k < k_h$ and $0 < \epsilon < \epsilon_b(k)$, then (2A.1) gives rise to bursting solutions.

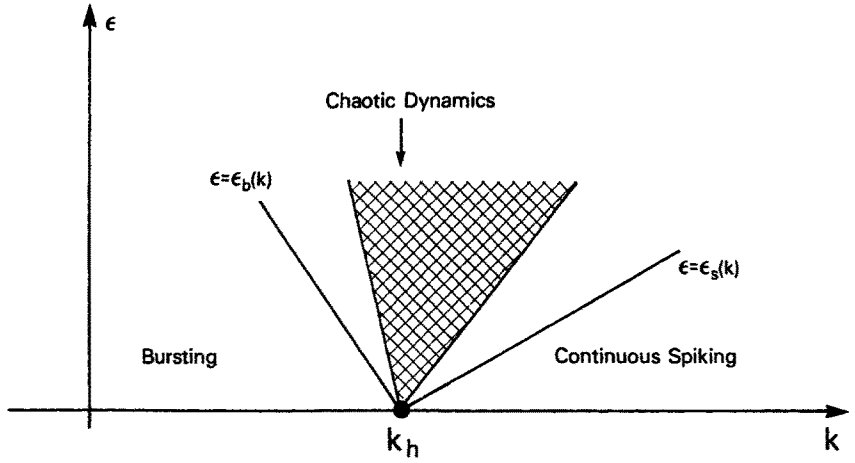

Fig. 6. The (k, ϵ) parameter plane. If $0 < k < k_h$ and $0 < \epsilon < \epsilon_b(k)$, then (2A.1) gives rise to bursting solutions, while if $k_h < k < k_0$ and $0 < \epsilon < \epsilon_s(k)$, then (2A.1) gives rise to continuous spiking. (2A.1) must give rise to chaotic dynamics for values of (k, ϵ) which lie between the curves $\epsilon = \epsilon_b(k)$ and $\epsilon = \epsilon_s(k)$.

If $k_h < k$ and $0 < \epsilon < \epsilon_s(k)$, then (2A.1) gives rise to continuous spiking. This is illustrated in Figure 6. We see in Figure 6 that there is a wedge-shaped region which lies between the curves $\epsilon = \epsilon_b(k)$ and $\epsilon = \epsilon_s(k)$. This region separates the values of the parameters where bursting and continuous spiking occur. This paper is primarily concerned with the dynamics associated with parameter values in this wedge-shaped region. We demonstrate that in this region, chaotic dynamics must arise.

B. Fibonacci Dynamics

In Section 3 we demonstrate that solutions of (2A.1) give rise to a two-dimensional map $\pi(\epsilon, k)$. The chaotic dynamics are described in terms of the properties of this map. It is well known that chaotic dynamics can arise from two-dimensional maps; the Smale horseshoe is perhaps the most famous example. The maps which we are interested in, however, are not topologically equivalent to the Smale horseshoe. They are topologically equivalent to other maps which we describe in this section.

Consider the squares $\Sigma_0 = [0, 1] \times [0, 1]$ and $\Sigma_1 = [-2, -1] \times [0, 1]$. Let $\Sigma = \Sigma_0 \cup \Sigma_1$. We define a map $\pi : \Sigma \to R^2$ as follows. As with the Smale horseshoe map, we think of π as performing a linear vertical expansion and a horizontal contraction of Σ_0 and Σ_1 followed by a folding. The foldings are such that $V_{00} \equiv \pi(\Sigma_0) \cap \Sigma_0$ consists of one vertical strip and $V_{01} \equiv \pi(\Sigma_0) \cap \Sigma_1$ consists of one vertical strip. See Figure 7. Moreover, $V_{10} \equiv \pi(\Sigma_1) \cap \Sigma_0$ consists of one vertical strip, and $\pi(\Sigma_1) \cap \Sigma_1$ is empty. We assume, for now, that restricted to $\Sigma \cap \pi^{-1}(\Sigma)$, the map is linear.

Note that $\pi^{-1}(V_{00})$ and $\pi^{-1}(V_{01})$ are horizontal strips which lie in Σ_0, while $\pi^{-1}(V_{10})$ is a horizontal strip which lies in Σ_1.

For $k \geq 1$, let $\Lambda^k = \{p \in \Sigma_0 : (\pi^k)^n(p) \in \Sigma_0 \text{ for each } n\}$. That is, Λ^k is the maximal invariant set of the map π^k restricted to Σ_0. We claim that for each

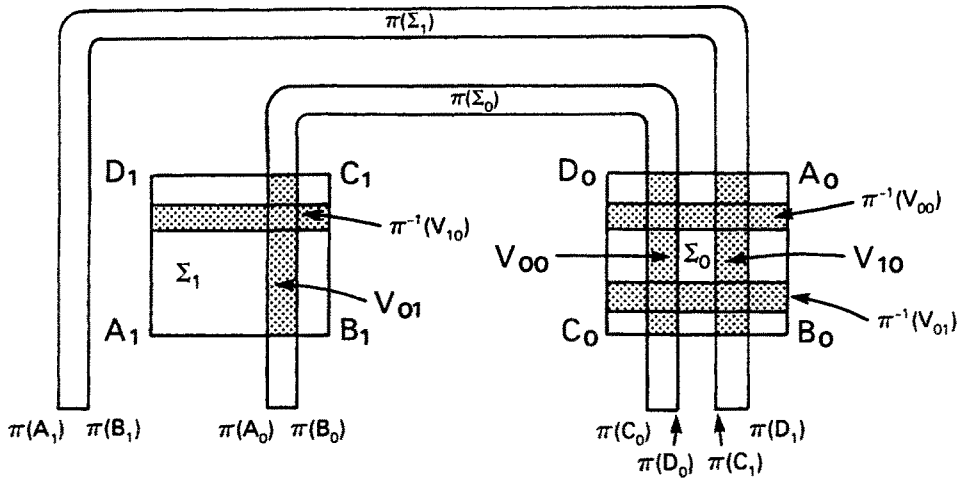

Fig. 7. A map, $\pi : \Sigma_0 \cup \Sigma_1 \to R^2$, which gives rise to Fibonacci dynamics. Note that $\pi(\Sigma_0)$ intersects both Σ_0 and Σ_1 along a verticle strip, while $\pi(\Sigma_1)$ only intersects Σ_0 along a verticle strip.

$k \geq 2$, Λ^k is a Cantor set. Moreover, the dynamics of π^k restricted to Λ^k can be described using the Fibonacci numbers. Therefore, let $\mathcal{F}_k$ be the k^{th} Fibonacci number. That is, $\mathcal{F}_0 = 1$, $\mathcal{F}_1 = 1$, and, for $k > 1$, $\mathcal{F}_k = \mathcal{F}_{k-1} + \mathcal{F}_{k-2}$. Let Γ_k be the set of bi-infinite sequences on $\mathcal{F}_k$ symbols.

Proposition 2B.1. For each $k \geq 1$ there is a one-to-one correspondence φ_k between Λ^k and Γ_k such that the sequence $b = \varphi_k(\pi^k(p))$ is obtained from the sequence $a = \varphi_k(p)$ by shifting one place $b_i = a_{i+1}$. Moreover, Λ^k is hyperbolic.

Remark. Each φ_k is actually a homeomorphism if we endow Λ^k and Γ_k with their natural topologies (see Guckenheimer and Holmes [8, pg. 233]).

We do not prove this proposition at this point; instead we state and prove a more general result in which we weaken the assumption that π, restricted to $\Sigma \cap \pi^{-1}(\Sigma)$, is linear. Our presentation is similar to that given in Guckenheimer and Holmes [8]. See also Moser [11].

Definition 2B.1. A vertical curve $x = v(y)$ in Σ_0 is a curve for which

$$0 \leq v(y) \leq 1, \quad |v(y_1) - v(y_2)| \leq \mu |y_1 - y_2| \quad \text{if} \quad 0 \leq y_1 \leq y_2 \leq 1$$

for some $0 < \mu < 1$. A horizontal curve $y = h(x)$ in Σ_0 is one for which

$$0 \leq h(x) \leq 1, \quad |h(x_1) - h(x_2)| \leq \mu |x_1 - x_2| \quad \text{if} \quad 0 \leq x_1 \leq x_2 \leq 1.$$

In a similar manner we can define a vertical curve in Σ_1 and a horizontal curve in Σ_1.

If $v_1(y) < v_2(y), y \in [0, 1]$, are two nonintersecting vertical curves in Σ_0, then we can define a vertical strip in Σ_0 as

$$V = \{(x, y) : x \in [v_1(y), v_2(y)], y \in [0, 1]\},$$

and if $h_1(x) < h_2(x), x \in [0, 1]$ are two nonintersecting horizontal curves in Σ_0, then we can define a horizontal strip in Σ_0 as

$$H = \{(x, y) : x \in [0, 1], y \in [h_1(x), h_2(x)]\}.$$

In a similar manner we can define a vertical strip in Σ_1 and a horizontal strip in Σ_1,

We now state the assumptions on the map $\pi : \Sigma \to R^2$

h1. There exist disjoint vertical strips V_{00} and V_{10} in Σ_0, a vertical strip V_{01} in Σ_1, horizontal strips H_{00} and H_{01} in Σ_0, and a horizontal strip H_{10} in Σ_1 with the following properties:
   (a) $\pi(\Sigma_0) \cap \Sigma_0 = (V_{00})$ and $\pi^{-1}(V_{00}) = H_{00}$,
   (b) $\pi(\Sigma_0) \cap \Sigma_1 = (V_{01})$ and $\pi^{-1}(V_{01}) = H_{01}$,
   (c) $\pi(\Sigma_1) \cap \Sigma_0 = (V_{10})$ and $\pi^{-1}(V_{10}) = H_{10}$,
   (d) $\pi(\Sigma_1) \cap \Sigma_1 = \varnothing$.

Let $V = V_{00} \cup V_{01} \cup V_{10}$ and $H = H_{00} \cup H_{01} \cup H_{10}$.

h2. There exist $\mu \in (0, \frac{1}{2})$ and sets (sector bundles) $S^u = \{(\xi, \eta) : |\xi| < \mu|\eta|\}$ defined over V and $S^s = \{(\xi, \eta) : |\eta| < \mu|\xi|\}$ defined over H such that $D\pi(S^u) \subset S^u$ and $D\pi^{-1}(S^s) \subset S^s$. Moreover, if $D\pi(\xi_0, \eta_0) = (\xi_1, \eta_1)$ and $D\pi^{-1}(\xi_0, \eta_0) = (\xi_{-1}, \eta_{-1})$, then $|\eta_1| \geq (1/\mu)|\eta_0|$ and $|\xi_{-1}| \geq (1/\mu)|\xi_0|$.

h3. If $p \in H$, then $|\det D\pi(p)|, |\det D\pi^{-1}(p)| \leq \frac{1}{2}\mu^{-2}$.

We can now state the main result of this section.

Proposition 2B.2. Assume that $\pi : \Sigma \to R^2$ satisfies (h1), (h2), and (h3). For $k \geq 1$, let Λ^k equal to the maximal invariant set of π^k restricted to Σ_0. Then Λ^k is topologically equivalent to a shift σ on Γ_k. Moreover, Λ^k is hyperbolic.

Proof. The proof is based on a theorem of Moser [11]; see also [8, Theorem 5.24]. This theorem, together with our assumptions, implies that the result follows once we prove that $\pi^k(\Sigma_0) \cap \Sigma_0$ is the union of $\mathcal{F}_k$ distinct vertical strips in Σ_0. (It is then clear that the preimage of these vertical strips under π^k consists of $\mathcal{F}_k$ horizontal strips in Σ_0.)

Let $a_0 = 1$. For $k \geq 1$, let a_k equal to the number of distinct vertical strips in $\pi^k(\Sigma_0) \cap \Sigma_0$, and let b_k equal to the number of distinct vertical strips in $\pi^k(\Sigma_0) \cap \Sigma_1$. From our assumptions it follows that $a_1 = b_1 = 1$. Moreover, since $\pi(\Sigma_0) \cap \Sigma_0$ and $\pi(\Sigma_1) \cap \Sigma_0$ each consists of one vertical strip in Σ_0, we conclude that $a_{k+1} = a_k + b_k$. Finally, since $\pi(\Sigma_0) \cap \Sigma_1$ consists of one vertical strip in Σ_1 and $\pi(\Sigma_1) \cap \Sigma_1 = \varnothing$, it follows that $b_{k+1} = a_k$. Hence, $a_{k+1} = a_k + b_k = a_k + a_{k-1}$, and the result follows.

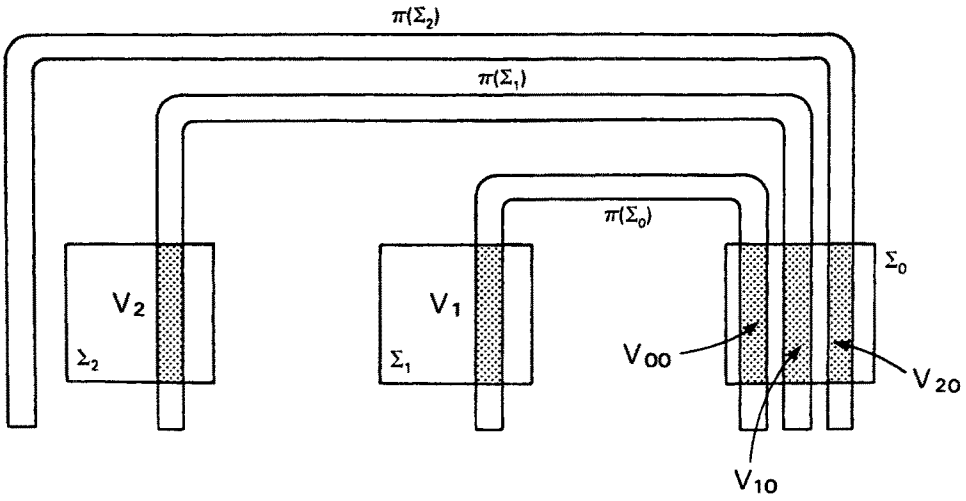

Fig. 8. A map, $\pi : \Sigma_0 \cup \Sigma_1 \cup \Sigma_2 \to R^2$, which gives rise to generalized Fibonacci dynamics.

We now generalize the preceding analysis to other maps. Fix $N \geq 0$, and let $\Sigma_0 = [0, 1] \times [0, 1]$ be as before. For $N > 0$ and $1 \leq j \leq N$, let $\Sigma_j = [-2j, -2j + 1] \times [0, 1]$.

Let $\Sigma = \cup_{j=0}^{N} \Sigma_j$. We now consider a map $\pi_N : \Sigma \to R^2$ with the following properties (see Figure 8):

a. If $0 \leq j \leq N$, then $\pi_N(\Sigma_j) \cap \Sigma_0 = V_{j0}$ is a vertical strip in Σ_0 and $\pi_N^{-1}(V_{j0}) = H_{j0}$ is a horizontal strip in Σ_j.
b. If $N > 0$ and $1 \leq j \leq N - 1$, then $\pi_N(\Sigma_j) \cap \Sigma_{j+1} = V_{j+1}$ is a vertical strip in Σ_{j+1} and $\pi_N^{-1}(V_{j+1}) = H_{j+1}$ is a horizontal strip in Σ_j.
c. If $N > 0, 0 \leq j \leq N$ and $k \notin \{0, j + 1\}$, then $\pi_N(\Sigma_j) \cap \Sigma_k = \varnothing$.
d. Let V and H be, respectively, the union of all the vertical and horizontal strips described in (a) and (b). Then (h2) and (h3) are satisfied with π replaced with π_N.

For $k \geq 1$, let Λ_N^k equal to the maximal invariant set of π_N^k restricted to Σ_0. We claim that Λ_N^k is a hyperbolic set which is topologically equivalent to the shift map on the set of bi-infinite sequences of $\mathcal{F}_N^k$ symbols. Here $\mathcal{F}_N^k$ is a generalized Fibonacci number which we now define.

If $N = 1$, then let $\mathcal{F}_N^k = 1$ for all k. If $N = 2$, then let $\mathcal{F}_N^k = \mathcal{F}_k$ be the usual Fibonacci numbers. Suppose that $\mathcal{F}_{N-1}^k$ has been defined for $N > 2$; we shall now define $\mathcal{F}_N^k$. If $0 \leq k \leq N$, let $\mathcal{F}_N^k = \mathcal{F}_{N-1}^k$. For $k > N$, let $\mathcal{F}_N^k = \sum_{j=1}^{N} \mathcal{F}_N^{k-j}$. That is, for $k > N$, $\mathcal{F}_N^k$ is the sum of the preceeding N generalized Fibonacci numbers.

Let Γ_N^k equal to the set of bi-infinite sequences on $\mathcal{F}_N^k$ symbols. We prove, in a manner similar to the proof of Propositions 3B.2, that Λ_N^k is topologically equivalent to the shift map on Γ_N^k. Our assumptions, together with Moser's Theorem, imply that it is only necessary to count the number of vertical strips in $\pi_N^k(\Sigma_0) \cap \Sigma_0$. For $0 \leq j \leq N$, let A_k^j equal to the number of distinct vertical strips in $\pi_N^k(\Sigma_0) \cap \Sigma_j$.

Certainly $A_0^0 = 1$, and $A_0^j = 0$ for $0 < j \leq N$. From (2B.1a) it follows that if $k > 0$, then $A_k^0 = \sum_{j=1}^N A_{k-1}^j$. From (2B.1b,c) it follows that if $k > 0$ and $1 < j \leq N$, then $A_k^j = A_{k-1}^{j-1}$. Therefore, if $k > N$, then

$$A_k^0 = \sum_{j=1}^N A_{k-1}^j = \sum_{j=1}^N A_{k-2}^{j-1} = \cdots = \sum_{j=1}^N A_{k-j}^0.$$

Using induction, we conclude that $A_k^0 = \mathcal{F}_N^k$.

Definition. We say that a map $\pi_N : \Sigma \to R^2$ which satisfies (2B.1) gives rise to N-Fibonacci dynamics.

Remark. If $N = 1$, then Λ_N^k is simply one point. This point corresponds to a periodic solution of π_N.

C. The Main Result

Throughout this section we assume that (A1)–(A6) are satisfied, $|k| < \delta_k$, and ϵ is sufficiently small. Our main result is stated in terms of a certain return map $\pi(\epsilon, k)$ which is defined in Section 3. This map is defined by solutions of (2A.1) near the homoclinic orbit $\gamma_h(t)$.

Theorem 2C.1. *Assume that (A1)–(A6) are satisfied and ϵ is sufficiently small. Then there exists an integer $N = N(\epsilon)$ and real numbers $\{k_j\}$, $1 \leq j \leq N(\epsilon)$, with the following properties:*

a. $-\delta_k < k_j < k_{j+1} < \delta_k$ *for each* j, $1 \leq j \leq N - 1$,
b. *for* $k \in [k_{2j-1}, k_{2j}]$, $\pi(\epsilon, k)$ *gives rise to* j*-Fibonacci dynamics,*
c. $N(\epsilon) \to \infty$ *as* $\epsilon \to 0$,
d. *each* $k_j \to k_h$ *as* $\epsilon \to 0$,
e. *when* $k = k_j$, $1 \leq j \leq N$, (2A.1) *gives rise to a homoclinic orbit.*

Remarks. (a) It is possible that $N(\epsilon) = \infty$. We do not consider this question, in detail, in this paper.

(b) Suppose that, after changing variables if necessary, both (A1)–(A6) and (H1)–(H8) are satisfied. Here, (H1)–(H8) are the assumptions listed in the Appendix that are required for the existence of bursting solutions and continuous spiking. Theorem A.1 implies that when $k = -\delta_k$ and ϵ is sufficiently small, (2A.1) gives rise to bursting solutions. When $k = +\delta_k$, (2A.1) gives rise to continuous spiking. Theorem 2C.1, therefore, describes how chaotic dynamics must arise during the transition from bursting to continuous spiking. The reason that there exist solutions such as those shown in Figure 1C is the following. Suppose that (k, ϵ) is chosen so that (2A.1) gives rise to Fibonacci dynamics, and let Λ be the maximal invariant set of the map $\pi(\epsilon, k)$. We shall see in the next section that Λ lies close to the homoclinic point q_0. That is, if U is any neighborhood of q_0, then, for ϵ sufficiently small, Λ must lie in

U. The results in [17] imply that if $\gamma(t)$ is any solution of (2A.1), then there must exist $\{t_j\}$ with $t_j \to \infty$ as $j \to \infty$ such that $\gamma(t_j) \in U$. Therefore, every solution of (2A.1) must lie close to Λ infinitely often. Near Λ, solutions of (2A.1) are extremely sensitive to initial conditions. In particular, the number of times which a typical trajectory winds around the upper branch before it falls to the lower branch depends very sensitively on initial conditions. Since each spike corresponds to the trajectory winding once around the upper branch, it is almost impossible to predict how many spikes the trajectory $\gamma(t)$ contains each time it passes close to the homoclinic point.

Figure 9 schematically illustrates our result. This figure displays the (k,ϵ) parameter space. When $(k,\epsilon) = (k_h, 0)$, (2A.1) gives to the homoclinic orbit $\gamma_h(t)$. Infinitely many wedge-shaped regions emanate from $(k_h, 0)$. We denote these sectors by S_1, $S_2, \ldots$. Each sector may only be defined for ϵ sufficiently small. Hence, each line segment $\epsilon = \epsilon_0$ may only intersect finitely many sectors. However, the number of sectors which the line segment $\epsilon = \epsilon_0$ intersects becomes unbounded as $\epsilon_0 \to 0$.

Now fix ϵ_0 sufficiently small. We begin at $(-\delta_k, \epsilon_0)$ and increase k until we reach (δ_k, ϵ_0). As we increase k, $\pi(\epsilon_0, k)$ gives rise to increasingly more complicated Fibonacci dynamics. In each odd sector S_{2j-1}, $\pi(\epsilon_0, k)$ gives rise to j-Fibonacci dynamics. In each even sector S_{2j}, $\pi(\epsilon_0, k)$ undergoes a transition from j- to $j+1$-Fibonacci dynamics. In these sectors, a large number of (global) bifurcations take place. We do not give a detailed description of the nature of these bifurcations in this paper.

As we increase k, (k, ϵ_0) eventually passes completely through the sectors $\{S_j\}$. This will happen for a value of k less than δ_k. There is then another transitional period until continuous spiking is achieved. During this transitional period, the dynamics must shed its complexity. We discuss this transition region in Section 4G.

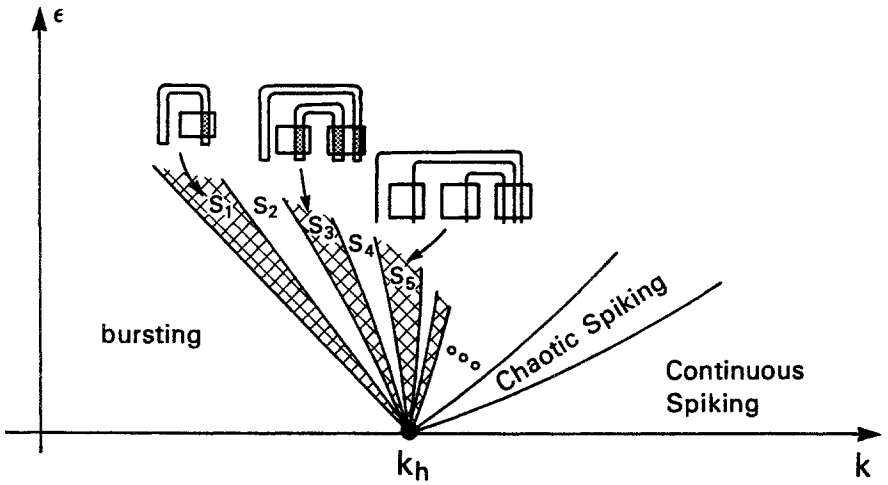

Fig. 9. The main result. The (k, ϵ) parameter plane is divided into countably many sectors. In each odd sector, S_{2j-1}, the map $\pi(\epsilon, k)$ gives rise to j-Fibonacci dynamics. The boundaries of each sector correspond to homoclinic solutions of (2A.1).

3. Flow-Defined Maps

A. Introduction

In this section we define the map $\pi(\epsilon, k)$ that appeared in the statement of Theorem 2C.1. This map is defined by solutions of (2A.1) near the homoclinic orbit $\gamma_h(t)$; it enables us to understand how solutions of (2A.1) near $\gamma_h(t)$ perturb for ϵ positive and k near 0. The map $\pi(\epsilon, k)$ is the composition of two other maps; that is, $\pi(\epsilon, k) = \psi(\epsilon, k) \circ \phi(\epsilon, k)$. The map $\varphi(\epsilon, k)$ is defined by the flow near the homoclinic point q_0. This map, for ϵ positive, is a singular perturbation from the case $\epsilon = 0$; however, by introducing local coordinates near q_0, we are able to express this map almost explicitly. The second map $\psi(\epsilon, k)$ is defined by the flow near $\gamma_h(t)$ but away from a small neighborhood of q_0. This map, for ϵ positive, is a regular perturbation from the case $\epsilon = 0$.

B. The Flow-Defined Map $\varphi(\epsilon, k)$

The map $\varphi(\epsilon, k)$ is defined by the flow in a small neighborhood of the homoclinic point q_0. We shall simplify matters by assuming that it is possible to change variables near q_0 so that in the new variables (2A.1) is of a simple linear form. This assumption will simplify the already tedious computations which follow. It is not difficult to see that the results carry over to the more general case; see Remark 5B.5.

We now briefly describe the changes of variables which transform (2A.1) to a simple linear form near q_0. Recall that each fixed point $q_y = (0, 0, y)$ is a saddle. Denote the positive and negative eigenvalues of (2A.1), linearized at q_y, by $\lambda_1(y)$ and $-\lambda_2(y)$, respectively. We may then change variables in the fast subsystem so that for (v, w, y) near q_0, (2A.1) becomes

$$\begin{aligned} x' &= \lambda_1(y)x + h.o.t., \\ z' &= -\lambda_2(y)z + h.o.t., \\ y' &= \epsilon \hat{g}(x, z, y, k). \end{aligned} \tag{3B.1}$$

Here, $\hat{g}(x, z, y, k) = g(v, w, y, k)$. By "h.o.t," we mean $\mathcal{O}(x^2 + z^2)$. We now introduce a new slow variable and rescale ϵ and k, for ϵ small and $|k| < \delta_k$, so that in the new variables (3B.1) becomes

$$\begin{aligned} x' &= \hat{\lambda}_1(u)x + h.o.t., \\ z' &= -\hat{\lambda}_2(u)z + h.o.t., \\ u' &= \epsilon(u + k) + \epsilon(h.o.t.). \end{aligned} \tag{3B.2}$$

In (3B.2), $\hat{\lambda}_i(u) = \lambda_i(y)$, $i = 1, 2$. By "h.o.t.," we now mean $\mathcal{O}(x^2 + z^2 + (u + k)^2)$. To simplify matters we drop the higher-order terms in (3B.2) and assume that, for $i = 1, 2$, $\hat{\lambda}_i(u) = \lambda_i(0) = \lambda_i$ are constant. The constants λ_1 and λ_2 are the same as in (A2). Therefore, we assume that for (v, w, y) near q_0, ϵ small and $|k| < \delta_k$, (2A.1) can be written in the form

$$\begin{aligned} x' &= \lambda_1 x, \\ z' &= -\lambda_2 z, \\ u' &= \epsilon(u + k). \end{aligned} \tag{3B.3}$$

We assume that these equations hold in some box

$$\mathcal{R} = \{(x, z, u) : |x| \leq \delta_x, |z| \leq \delta_z, |u| \leq \delta_u\}. \tag{3B.4}$$

Restrictions on the constants δ_x, δ_z, and δ_u are given as we go along.

We assume, without loss of generality, that the homoclinic orbit $\gamma_h(t)$ leaves $\mathcal{R}$ through its "front" face

$$\mathcal{F} = \{(x, z, u) \in \mathcal{R} : x = \delta_x\},$$

and $\gamma_h(t)$ enters $\mathcal{R}$ through its "top" face

$$\mathcal{T} = \{(x, z, u) \in \mathcal{R} : z = \delta_z\}.$$

It will be necessary to consider the following subsets of the boundary of $\mathcal{R}$:

$$\begin{aligned} \mathcal{F}' &= \{(x, z, u) \in \mathcal{F} : z > 0\}, \\ \mathcal{T}' &= \{(x, z, u) \in \mathcal{T} : x > 0\}, \\ \mathcal{R}' &= (x, z, u) \in \partial\mathcal{R} : 0 < x, 0 < z\}. \end{aligned}$$

We assume throughout the remainder of this section that ϵ is sufficiently small and $|k| < \delta_u$. Then $\varphi(\epsilon, k) : \mathcal{T}' \to \mathcal{R}'$ is defined as follows. Fix $\gamma_0 \in \mathcal{T}'$, and let $\gamma(t)$ be the solution of (3B.3) with $\gamma(0) = \gamma_0$. There must exist $t_0 > 0$ such that $\gamma(t) \in \mathcal{R}$

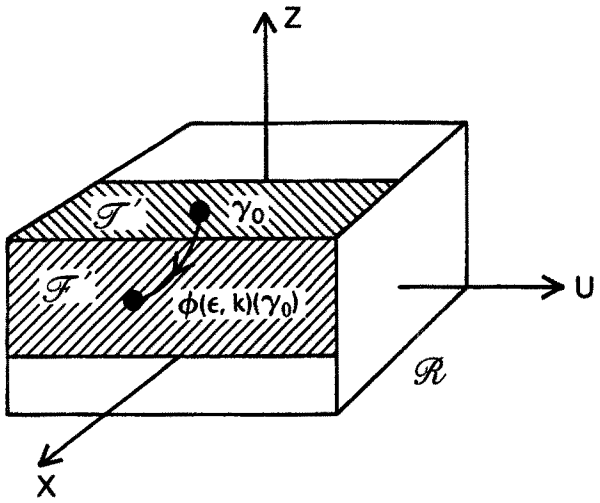

Fig. 10. The map $\phi(\epsilon, k)$. This map is defined by solutions of (2A.1) near the fixed point q_k. When $\epsilon = 0$, $\phi(\epsilon, k)$ maps $\mathcal{T}'$ onto $\mathcal{F}'$.

for $t \in (0, t_0)$ and $\gamma(t_0) \in \mathcal{R}'$. We set $\varphi(\epsilon, k)(\gamma_0) = \gamma(t_0)$. See Figure 10. This defines a smooth map from $\mathcal{T}'$ onto $\mathcal{R}'$. Let

$$T(\epsilon, k) = \varphi(\epsilon, k)^{-1}(\mathcal{F}').$$

It is not hard to show that $T(\epsilon, k) \to \mathcal{T}'$ as $\epsilon \to 0$.

Since (3B.3) is of such a simple form, we can express $\varphi(\epsilon, k)$ explicitly. A simple calculation shows that if $(x, \delta_z, u) \in T(\epsilon, k)$, then

$$\varphi(\epsilon, k)(x, \delta_z, u) = (\delta_x, \varphi_z(x, u), \varphi_u(x, u)) \tag{3B.6a}$$

where

$$\varphi_z(x, u) = \delta_z \left(\frac{x}{\delta_x}\right)^{\lambda_2/\lambda_1} \quad \text{and} \quad \varphi_u(x, u) = -k + [u + k]\left[\frac{\delta_x}{x}\right]^{\epsilon/\lambda_1}. \tag{3B.6b}$$

We will be particularly interested in the image, under $\varphi(\epsilon, k)$, of a line segment of the form

$$\ell = \{(x, \delta_z, u) \in \mathcal{T}' : x = m(u - b)\}.$$

Here, $|b| < \delta_u$, and $m \neq 0$. A straightforward computation shows that $\varphi(\epsilon, k)(\ell) \cap \mathcal{F}$ is a curve which can be written as

$$\varphi(\epsilon, k)(\ell) \cap \mathcal{F} = \{(\delta_x, z, u) \in \mathcal{F} : u = h(z)\}$$

where

$$h(z) = -k + [b + k]\left[\frac{z}{\delta_z}\right]^{-\epsilon/\lambda_2} + \frac{\delta_x}{m}\left(\frac{z}{\delta_z}\right)^{\lambda_1 - \epsilon/\lambda_2} \tag{3B.7}$$

The curve $u = h(z)$ is illustrated in Figure 11. Note that the qualitative features of this curve depend on whether $k < -b, k = -b$, or $k > -b$, and whether $\lambda_1 < \lambda_2$ or $\lambda_1 > \lambda_2$. If $k < -b$, then $h(z)$ is an increasing function, while if $k > -b$, then $h(z)$ has a unique local minimum. If $k = -b$ and $\lambda_1 < \lambda_2$, then this curve is tangent to the u-axis at the point $(u, z) = (-k, 0)$. If $k = -b$ and $\lambda_1 > \lambda_2$, then this curve has a vertical tangent at $(u, z) = (-k, 0)$. These qualitative differences play a crucial role in the analysis which follows.

We conclude this subsection with some simple observations concerning the map $\varphi(\epsilon, k)$. The following result follows from the explicit formula for $\varphi(\epsilon, k)$ given in (3B.6). Let $\varphi_z(x, u)$ and $\varphi_u(x, u)$ be the maps defined in (3B.6b).

Lemma 3B.1. *Assume that* $p_1 = (x^1, \delta_z, u^1)$ *and* $p_2 = (x^2, \delta_z, u^2)$ *both lie in* $T(\epsilon, k)$. *If* $x^1 < x^2$, *then* $\varphi_z(x^1, u^1) < \varphi_z(x^2, u^2)$. *If* $x^1 = x^2$ *and* $u^1 < u^2$, *then* $\varphi_u(x^1, u^1) < \varphi_u(x^2, u^2)$.

The following two corollaries are immediate consequences of the preceding lemma.

Corollary 3B.2. *Assume that* $\hat{\alpha} = \{(x, \delta_z, u) \in \mathcal{T}' : u = \alpha(x)\}$ *is a smooth curve in* $\mathcal{T}'$. *Then* $\hat{\beta} \equiv \varphi(\epsilon, k)(\hat{\alpha}) \cap \mathcal{F}$ *is a smooth curve in* $\mathcal{F}'$ *which can be written in the form* $\hat{\beta} = \{(\delta_x, z, u) \in \mathcal{F}' : u = \beta(z)\}$.

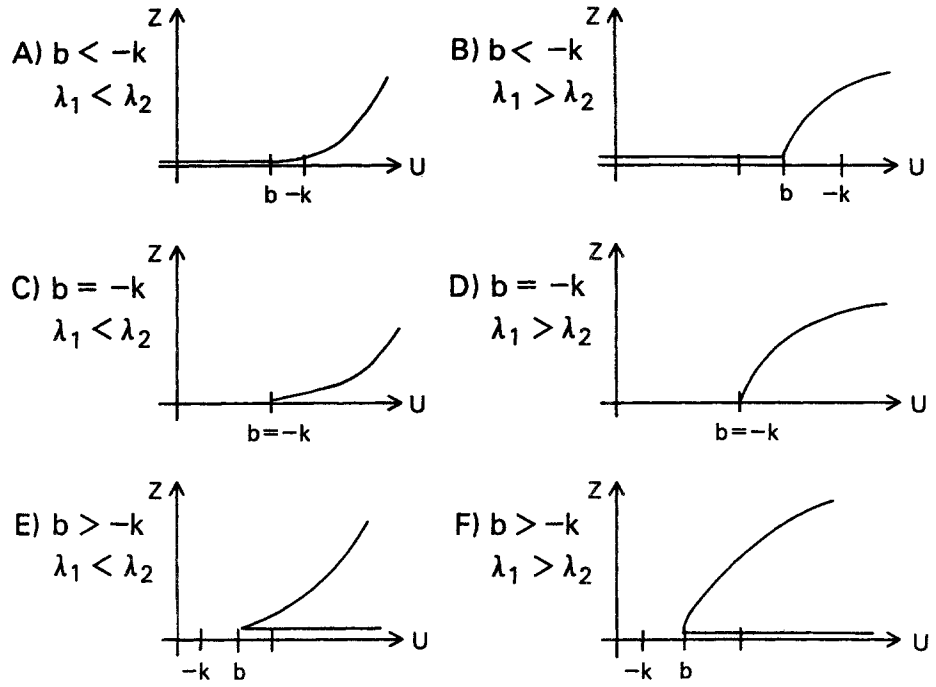

Fig. 11. The function $u = h(z)$ given by (3B.7). If $k < -b$, then $h(z)$ is increasing. If $k > -b$, then $h(z)$ has a unique minimum. If $k = -b$ and $\lambda_1 < \lambda_2$, then this function has a horizontal tangent at $(u, z) = (-k, 0)$. If $k = -b$ and $\lambda_1 > \lambda_2$, then this tangency is vertical.

Corollary 3B.3. *Assume that* $\hat{\alpha}_i = \{(x, \delta_z, u) : u = \alpha_i(x)\}, i = 1, 2,$ *define smooth curves in* $\mathcal{T}'$ *such that* $\alpha_1(x) < \alpha_2(x)$ *for each* x. *Let* $\hat{\beta}_i \equiv \varphi(\epsilon, k)(\hat{\alpha}_i) \cap \mathcal{F} = \{(\delta_x, z, u) \in \mathcal{F}' : u = \beta_i(z)\}$. *Then* $\beta_1(z) < \beta_2(z)$ *for each* z *for which* $\beta_1(z)$ *and* $\beta_2(z)$ *are both defined.*

We also need the following result.

Lemma 3B.4. *Assume that* $\hat{\alpha} = \{(x, \delta_z, u) \in T' : u = \alpha(x)\}$ *is a smooth curve in* $\mathcal{T}$ *such that* $\alpha(0) < -k$ *and* $\alpha'(x) > 0$ *for each* x. *Then, for* ϵ *sufficiently small,* $\hat{\beta} = \varphi(\epsilon, k)(\hat{\alpha}) \cap \mathcal{F}'$ *can be written as* $\hat{\beta} = \{(\delta_x, z, u) \in \mathcal{F}' : z = \beta(u)\}$. *Here,* $\beta(u)$ *is an increasing function defined for* $u \in (-\delta_u, \beta_0)$ *for some* $\beta_0 \in (-\delta_u, \delta_u)$.

Proof. This result is proved by considering the linearization of the map $\varphi(\epsilon, k)$. The linearization can be computed explicitly using (3B.6). The details of this computation are straightforward but somewhat tedious, so we do not give the details. The reason that the last statement in the lemma is true is that the assumption that $\alpha(0) < -k$ implies that

$$\varphi(\epsilon, k)(0, \delta_z, \alpha(0)) \in \{(x, z, u) \in \partial\mathcal{R} : u = -\delta_u\}.$$

C. The Flow-Defined Map $\psi(\epsilon, k)$

The map $\psi(\epsilon, k)$ is a diffeomorphism from a subset of $\mathcal{F}$ into $\mathcal{T}$. Since $\psi(\epsilon, k)$ is a regular perturbation from the case $\epsilon = 0$, we consider this case first. Throughout this discussion we assume that $|k| < \delta_u$. Recall than when $\epsilon = 0$, the homoclinic orbit $\gamma_h(t)$ leaves $\mathcal{R}$ through $\mathcal{F}$ and then enters $\mathcal{R}$ through $\mathcal{T}$. This homoclinic orbit intersects $\mathcal{F}$ at the point $(\delta_x, 0, 0)$ and intersects $\mathcal{T}$ at the point $(0, \delta_z, 0)$. Therefore, when $\epsilon = 0$, the flow defines a diffeomorphism from a small neighborhood of $(\delta_x, 0, 0)$ in $\mathcal{F}$ onto a small neighborhood of $(0, 0, \delta_z)$ in $\mathcal{T}$. We denote this map by $\psi(0, k)$, even though it does not actually depend on k. By continuous dependence of solutions of an ordinary differential equation on a parameter, this map perturbs to a diffeomorphism for ϵ sufficiently small. More precisely, choose $\gamma_0 \in \mathcal{F}$, and let $\gamma(t)$ be the solution of (2A.1) with $\gamma(0) = \gamma_0$. If $\|\gamma_0 - (\delta_x, 0, 0)\|$ and ϵ are sufficiently small, then there must exist $t_0 > 0$ such that $\gamma(t) \notin \mathcal{R}$ for $0 < t < t_0$ and $\gamma(t_0) \in \mathcal{T}$. We define $\psi(\epsilon, k)$ by $\psi(\epsilon, k)(\gamma_0) = \gamma(t_0)$. Of course, $\psi(\epsilon, k)$ may only be defined on a subset of $\mathcal{F}$. However, if δ_x is fixed, then it is possible to choose δ_z and δ_u so small that, for ϵ sufficiently small, $\psi(\epsilon, k)$ defines a diffeomorphism from

$$\mathcal{F}_0 = \left\{ (\delta_x, z, u) \in \mathcal{F} : |u| \leq \frac{1}{2}\delta_u \right\} \tag{3C.1}$$

into $\mathcal{T}$. Note that ψ depends smoothly on ϵ and k, even up to $\epsilon = 0$.

We now wish to estimate $D\psi(\epsilon, k)$, the linearization of $\psi(\epsilon, k)$. In what follows, we assume that

$$\psi(\epsilon, k)(\delta_x, z, u) = (\psi_x(z, u), \delta_z, \psi_u(z, u)), \tag{3C.2}$$

and let $\hat{\psi}(\epsilon, k)(z, u) = (\psi_x(z, u), \psi_u(z, u))$. Of course, the functions ψ_x and ψ_u also depend on ϵ and k; however, in order to simplify the notation, we do not express this dependence explicitly.

Since $\hat{\psi}(\epsilon, k)$ is a regular perturbation of $\psi(0, k)$, we first consider the case $\epsilon = 0$. Let $p = (\delta_x, z, u) \in \mathcal{F}_0$. The last equation in (2A.1) implies that if $\epsilon = 0$, then $\psi_u(z, u) = u$. Therefore, if $\epsilon = 0$, then

$$\frac{\partial \psi_u}{\partial z} = 0 \quad \text{and} \quad \frac{\partial \psi_u}{\partial u} = 1. \tag{3C.3}$$

In order to compute the partial derivatives of ψ_x, we use (A3) which states that W^{cu} and W^{cs} intersect transversely. From (3B.3) it follows that

$$\begin{aligned} \ell_u &\equiv W^{cu}_{loc} \cap \mathcal{F} = \{(\delta_x, z, u) \in \mathcal{F} : z = 0\}, \\ \ell_s &\equiv W^{cs}_{loc} \cap \mathcal{T} = \{(x, \delta_z, u) \in \mathcal{T} : x = 0\}. \end{aligned} \tag{3C.4}$$

The assumption that W^{cu} and W^{cs} intersect transversely implies that there exists a smooth function $x = h(u)$ with $h(0) = 0$ and $h'(0) = m \neq 0$ such that

$$\psi(0, k)(\ell_u) = \{(x, \delta_z, u) \in \mathcal{T} : u = h(x)\}. \tag{3C.5}$$

Note that (A4), together with our assumption that $\gamma_h(t)$ leaves $\mathcal{R}$ through $\mathcal{F}$, implies that $m > 0$. Together with (3C.4), it now follows that $(\partial \psi_x / \partial u)(0, 0) = 1/m > 0$.

Finally, let $\beta = (\partial\psi_x/\partial z)(0,0)$. Clearly, $\beta \neq 0$. In fact, it is not hard to see that $\beta > 0$. We have now demonstrated that when $\epsilon = 0$ and $(x, u) = (0,0)$,

$$D\hat{\psi}(0,k) = \begin{bmatrix} \dfrac{\partial\psi_x}{\partial z}(0,0) & \dfrac{\partial\psi_x}{\partial u}(0,0) \\ \dfrac{\partial\psi_u}{\partial z}(0,0) & \dfrac{\partial\psi_u}{\partial u}(0,0) \end{bmatrix} = \begin{bmatrix} \beta & 1/m \\ 0 & 1 \end{bmatrix}. \tag{3C.6}$$

The following result now follows because $\psi(\epsilon, k)(p)$ depends smoothly on each of its arguments.

Proposition 3C.1. Fix $\delta > 0$. The constants δ_x, δ_z, and δ_u can be chosen so that if ϵ is sufficiently small and $(\delta_x, z, u) \in \mathcal{F}_0$, then

$$\sup\left\{\left|\frac{\partial\psi_x}{\partial z}(z,u) - \beta\right|, \left|\frac{\partial\psi_x}{\partial u}(z,u) - \frac{1}{m}\right|, \left|\frac{\partial\psi_u}{\partial_z}(z,u)\right|, \left|\frac{\partial\psi_u}{\partial u}(z,u) - 1\right|\right\} < \delta.$$

A consequence of this proposition is that δ_x, δ_z, andδ_u can be chosen so that, for ϵ sufficiently small, the following result holds:

Corollary 3C.2. *Assume that $z = \alpha(u)$ is a smooth function such that $\alpha'(u) \geq 0$ for each u and $\hat{\alpha} = \{(\delta_x, z, u) \in \mathcal{F}_0 : z = \alpha(u)\}$ defines a smooth curve in $\mathcal{F}_0$. Then $\hat{\beta} = \psi(\epsilon, k)(\hat{\alpha})$ is a smooth curve in $\mathcal{T}$ which can be written as $\hat{\beta} = \{(x, \delta_z, u) \in \mathcal{T} : u = \beta(x)\}$. Moreover, $\beta'(x) > 0$ for each x.*

Remark 3C.3. The maps $\psi(\epsilon, k)$ preserve a natural ordering of curves in $\mathcal{F}_0$. By this we mean the following: Suppose that $\hat{\alpha}_1$ and $\hat{\alpha}_2$ are smooth curves in $\mathcal{F}_0$ defined by $\hat{\alpha}_i = \{(\delta_x, z, u) \in \mathcal{F}_0 : z = \alpha_i(u)\}$, $i = 1, 2$. Assume that for each u, $\alpha_1(u) < \alpha_2(u)$ and $\alpha_i'(u) \geq 0$, $i = 1, 2$. Let $\hat{\beta}_i = \psi(\epsilon, k)(\hat{\alpha}_i) = \{(x, \delta_z, u) \in T : u = \beta_i(x)\}$. We claim that $\beta_1(x) \geq \beta_2(x)$ for each x for which each function is defined. This follows easily because the union of all of the trajectories through points in $\hat{\alpha}_1$ and $\hat{\alpha}_2$ defines two smooth manifolds which cannot intersect. It is impossible for one of these manifolds to "wrap around" the other. One can extend this remark to more general curves; the assumption that $\alpha_i'(u) \geq 0$, for example, is not really necessary.

We conclude this section with the following important result.

Proposition 3C.4. For each ϵ sufficiently small, there exists $k = k(\epsilon)$ such that $|k(\epsilon)| < \frac{1}{2}\delta_u$ and (2A.1) gives rise to a homoclinic orbit.

Proof. For $\epsilon > 0$ and $|k| < \delta_u$, let q_k be the unique fixed point of (2A.1). Let $W^s = W^s(\epsilon, k)$ and $W^u = W^u(\epsilon, k)$ be the stable and unstable manifolds of q_k, respectively. We need to prove that if ϵ is sufficiently small, then there exists k with $|k| < \frac{1}{2}\delta_u$ such that $W^s(\epsilon, k) \cap W^u(\epsilon, k) \neq \varnothing$. It follows from (3B.3) that $W^u_{loc}(\epsilon, k) = W^{cu}$. Moreover, if ℓ_u is as in (3C.4), then

$$\begin{aligned} W^u_{loc}(\epsilon, k) \cap \mathcal{F} &= \ell_u = \{(\delta_x, z, u) \in \mathcal{F} : z = 0\}, \\ W^s_{loc}(\epsilon, k) \cap \mathcal{T} &= \{(0, \delta_z, -k)\} \equiv p_k. \end{aligned} \tag{3C.7}$$

Therefore, it suffices to prove that for each ϵ sufficiently small, there exists k, with $|k| < \frac{1}{2}\delta_u$, such that $p_k \in \psi(\epsilon, k)(\ell_u)$.

Recall, from (3C.5), that $\psi(0, k)(\ell_u)$ defines a smooth curve, which we denote by $\hat{H}(0, k)$, in $\mathcal{T}$. Since $\psi(\epsilon, k)$ depends smoothly on each of its arguments it follows that if ϵ is sufficiently small, then $\psi(\epsilon, k)(\ell_u)$ defines a smooth curve $\hat{H}(\epsilon, k)$ in $\mathcal{T}$. Moreover, from Corollary 3C.2, we can write $\hat{H}(\epsilon, k)$ as

$$\hat{H}(\epsilon, k) = \{(x, \delta_z, u) \in \mathcal{T} : u = H(\epsilon, k)(x)\}. \tag{3C.8}$$

Here, $H(\epsilon, k)(x)$ is a smooth function such that $H(\epsilon, k)(x) \to H(0, k)(x)$ uniformly as $\epsilon \to 0$. In particular, $H(\epsilon, k)(0) \to H(0, k)(0) = 0$ as $\epsilon \to 0$. Therefore, there exists ϵ_0 such that if $0 < \epsilon < \epsilon_0$ and $|k| \leq \frac{1}{2}\delta_u$, then $|H(\epsilon, k)(0)| < \frac{1}{2}\delta_u$.

We have now shown that if $0 < \epsilon < \epsilon_0$, then $H(\epsilon, \frac{1}{2}\delta_u)(0) > -\frac{1}{2}\delta_u$ and $H(\epsilon, -\frac{1}{2}\delta_u)(0) < \frac{1}{2}\delta_u$. It then follows that there exists $k = k(\epsilon)$ such that $|k(\epsilon)| < \frac{1}{2}\delta_u$ and $H(\epsilon, k(\epsilon))(0) = -k(\epsilon)$. This completes the proof because we have now shown that the point $(0, \delta_z, -k(\epsilon))$ lies in both $W^u(\epsilon, k(\epsilon))$ and $W^s(\epsilon, k(\epsilon))$.

Remarks. (a) The existence of this homoclinic orbit does not depend on the assumption A2.

(b) The homoclinic orbit obtained in the preceding Proposition has winding number one in the sense that its trajectory in phase space "winds around" the upper branch just once. Another way to say this is that its trajectory intersects $\mathcal{F}$ or $\mathcal{T}$ just once. In the next section we demonstrate that if $\lambda_1 < \lambda_2$ (that is, (A2) is satisfied), then (2A.1) gives rise to many more homoclinic orbits as the parameter k is varied. These homoclinic orbits can be characterized by their winding number.

(c) It is possible that $k(\epsilon)$ is not the only solution of the equation $H(\epsilon, k(\epsilon))(0) = -k(\epsilon)$. However, in order to avoid further notation we assume that $k(\epsilon)$ is the unique solution. There is no difficulty in adjusting the proof of Theorem 2C.1 if this is not the case. Note that

$$H(\epsilon, k)(0) < -k \quad \text{if and only if} \quad k < k(\epsilon). \tag{3C.9}$$

D. The Flow-Defined Map $\pi(\epsilon, k)$

As before, we assume that ϵ is sufficiently small and $|k| < \frac{1}{2}\delta_u$. Let $\pi(\epsilon, k) = \psi(\epsilon, k) \circ \varphi(\epsilon, k)$. There is no problem in showing that the domain of $\pi(\epsilon, k)$ is nonempty. In fact, for each k,

$$\operatorname{dom}\pi(0, k) \supset \left\{(x, \delta_z, y) \in \mathcal{T} : x > 0, |u| < \frac{1}{2}\delta_u\right\},$$

and $\operatorname{dom}\pi(\epsilon, k) \to \operatorname{dom}\pi(0, k)$, in an obvious uniform sense, as $\epsilon \to 0$. We shall abuse notation, slightly, as follows: Suppose that $D \subset \mathcal{T}$. By $\pi(\epsilon, k)(D)$ we mean $\pi(\epsilon, k)(D \cap \operatorname{dom}\pi(\epsilon, k))$.

In this section we state a very important result. The statement and proof of this result are quite technical; however, once we have this result, the analysis of the chaotic dynamics, as described in Theorem 2C.1, will be straightforward. In this section we shall try to motivate and then state the result. In the next section we show how it is used to prove Theorem 2C.1. The proof of the result is given in Section 5.

We now try to motivate the statement of the following proposition. Perhaps the most important ingredient in the proof of Theorem 2C.2 is to keep track of $W^u_{q_k}$, the unstable manifold of the fixed point q_k, as it loops around in phase space. Trajectories in $W^u_{q_k}$ which lie close to the original homoclinic orbit $\gamma_h(t)$ may wind around the upper branch many times. These trajectories cross the set $\mathcal{T}$ many times. Now recall that $\dim W^u_{q_k} = 2$. Therefore, each time that $W^u_{q_k}$ loops around the upper branch it will intersect $\mathcal{T}$ along a curve, or possibly several curves. These curves partition $\mathcal{T}$ into several sectors. From these sectors, we will construct the sets corresponding to Σ_j, $j = 0, 1, \ldots$, that appeared in Section 2B.

In the following proposition we begin with a curve $\hat{\alpha}$ in $\mathcal{T}'$ and analyze the image $\pi(\epsilon, k)(\hat{\alpha}) \cap \mathcal{T}'$. When we apply this proposition in the later sections, $\hat{\alpha}$ will correspond to one of the curves in $W^u_{q_k} \cap \mathcal{T}'$. An important consequence of the following proposition is that $\pi(\epsilon, k)(\hat{\alpha}) \cap \mathcal{T}'$ may consist of two curves. When we discuss the proof of the proposition in Section 5, we will see that the reason that there are two curves is because of the stretching and folding properties of the map $\pi(\epsilon, k)$. These properties are, of course, crucial to the existence of the chaotic dynamics.

In the statement of the following proposition, let $\hat{H}(\epsilon, k)$ and $H(\epsilon, k)$ be as in (3C.8), and let $k(\epsilon)$ be as in Proposition 3C.4. Recall that $H(\epsilon, k(\epsilon))(0) = -k(\epsilon)$. Let λ_1 and λ_2 be as in (A2), and let m be as in Proposition 3C.1. We always assume that $|k| < \frac{1}{2}\delta_u$ and ϵ is sufficiently small. In what follows, the constants C_i, $i = 0, 1, \ldots$, do not depend on ϵ or k. We set

$$\lambda = \frac{\lambda_2 - \lambda_1}{5} \quad \text{and} \quad r = \left(\frac{\lambda_2 - \lambda_1 - 2\lambda}{\lambda_1}\right)\lambda_2. \tag{3D.1}$$

Proposition 3D.1. Assume that (A1)–(A6) are satisfied. Then there exist positive constants C_0, C_1, C_2, C_3, and C_4 with the following properties: Suppose that $0 < H(\epsilon, k)(0) + k < \epsilon^{(\lambda_2 - \lambda)/\lambda_1}$ and $\epsilon C_1 < C < C_0$. Assume that $u = \alpha(x)$ is a smooth function which satisfies $-k < \alpha(0) < H(\epsilon, k)(0)$ and $(m/2) < \alpha'(x) < 2m$ for $0 \le x \le C$. Let

$$\hat{\alpha} = \{(x, \delta_z, u) \in \mathcal{T} : u = \alpha(x) \quad \text{for} \quad 0 < x < C\}.$$

Then $\pi(\epsilon, k)(\hat{\alpha}) \cap \mathcal{T}' = \hat{\alpha}_1 \cup \hat{\alpha}_2$ where $\hat{\alpha}_1$ and $\hat{\alpha}_2$ are disjoint, smooth curves which can be expressed as

$$\hat{\alpha}_i = \{(x, \delta_z, u) \in \mathcal{T}' : u = \alpha_i(x)\}, \quad i = 1, 2.$$

Moreover, $0 < C_2 < 1$ and

a. $\alpha_1(x)$ is defined for $0 \le x < C_2 C$,
b. $(m/2) < \alpha_1'(x) < 2m$ for $0 \le x < C_2 C$,
c. $\alpha_2(x)$ is defined for $0 \le x \le C_0$,
d. $(m/2) < \alpha_2'(x) < 2m$ for $0 \le x \le C_0$, (3D.2)
e. $\alpha_1(x) < \alpha_2(x) < H(\epsilon, k)(x)$ for $0 \le x < C_2 C$,
f. $H(\epsilon, k)(0) - C_3\epsilon^{\lambda_2/\lambda_1} < \alpha_1(0) < H(\epsilon, k)(0) - C_4\epsilon^{\lambda_2/\lambda_1}$,
g. $H(\epsilon, k)(0) - [H(\epsilon, k)(0) + k]\epsilon^{r/\epsilon} < \alpha_2(0) < H(\epsilon, k)(0)$.

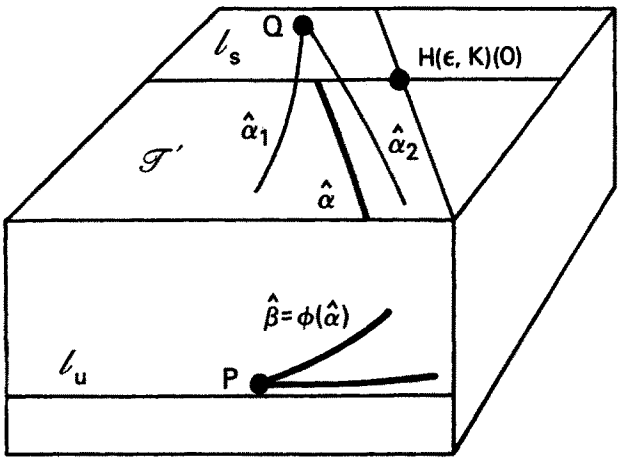

Fig. 12. Objects which appear in the statement of Proposition 3D.1. Here, $\hat{\beta} = \phi(\epsilon, k)(\hat{\alpha})$ and $\varphi(\epsilon, k)(\hat{\beta}) \cap \mathcal{T}' = \hat{\alpha}_1 \cup \hat{\alpha}_2$. The point P is the vertex of $\hat{\beta}$ and $Q = \varphi(\epsilon, k)(P)$. Note that $Q \notin \mathcal{T}'$.

In Figure 12 we illustrate some of the objects which appear in the statement of Proposition 3D.1. The most boldly drawn curves in Figure 12 are $\hat{\alpha}$ and $\hat{\beta} = \phi(\epsilon, k)(\hat{\alpha})$. Note that $\hat{\beta}$ resembles the curve $u = h(z)$ in Figure 11E. This is to be expected since $-k < \alpha(0)$ and $\lambda_1 < \lambda_2$. The point labeled P corresponds to the vertex of the curve $\hat{\beta}$. Here $Q = \psi(\epsilon, k)(P)$ is the vertex of the curve $\psi(\epsilon, k)(\hat{\beta}) = \pi(\epsilon, k)(\hat{\alpha})$. It is crucial to our analysis that Q lies in the set $\{(x, \delta_z, u) \in \mathcal{T} : x < 0\}$. That is, $Q \notin \mathcal{T}'$. From this, it follows that $\pi(\epsilon, k)(\hat{\alpha}) \cap \mathcal{T}'$ consists of two disjoint curves; these are denoted by $\hat{\alpha}_1$ and $\hat{\alpha}_2$ in the Proposition and Figure 12. We note that the properties of $\hat{\alpha}_1$ and $\hat{\alpha}_2$ described in (3D.2) guarantee that we can apply the proposition again with $\hat{\alpha}$ replaced with either $\hat{\alpha}_1$ or $\hat{\alpha}_2$.

4. Transition to Continuous Spiking

A. Introduction

Throughout this section we assume that ϵ is sufficiently small, $|k| < \frac{1}{2}\delta_u$, and Proposition 3D.1 holds. We demonstrate how Proposition 3D.1 is used in the proof of Theorem 2C.1. The key ingredient in understanding how the chaotic dynamics arise to follow the unstable manifold, $W^u(\epsilon, k)$, of the fixed point q_k as it loops around in phase space. This manifold intersects the faces $\mathcal{F}$ and $\mathcal{T}$ of $\mathcal{R}$ a large number of times. Each intersection defines a curve in $\mathcal{F}$ or $\mathcal{T}$. It will be necessary to determine how the qualitative features of these curves change as k is varied.

Since ϵ is assumed to be fixed throughout this section, we drop the dependence on ϵ in our notation. Hence, we let $\pi(k)(\cdot) = \pi(\epsilon, k)(\cdot)$, $W^u(k) = W^u(\epsilon, k)$, and so on.

Let $\ell_u = W^u_{loc}(k) \cap \mathcal{F}$ and $p_k = W^s_{loc}(k) \cap \mathcal{T}$ be as in (3C.7). Let $G^0 = \ell_u$ and $H^0(k) = \psi(k)(G_0) \cap \mathcal{T}'$. We then define recursively for $j \geq 1, G^j(k) = \varphi(k)(H^{j-1}(k)) \cap \mathcal{F}_0$ and $H^j(k) = \psi(k)(G^j(k)) \cap \mathcal{T}'$. This defines, for some integer $N(\epsilon, k)$, two finite sequences of sets $\{H^j(k)\}$ and $\{G^j(k)\}, 0 \leq j \leq N(\epsilon, k)$. Note that each $H^j(k)$ or $G^j(k)$ may be a union of many curves in $\mathcal{T}$ or $\mathcal{F}$, respectively. In what follows we describe the qualitative features of these sets, in detail. We will drop the dependence on k in our notation if the value of k is understood.

B. The Case: $k < k(\epsilon)$

Let $k(\epsilon)$ be as in Proposition 3C.4, and assume that $-\frac{1}{2}\delta_u < k < k(\epsilon)$. If the assumptions H1–H8 are satisfied, then for these values of the parameters, (2A.1) will give rise to bursting solutions; (2A.1) does not give rise to the Fibonacci-type dynamics described in Section 2B. We note that even if $k < k(\epsilon)$, then the horseshoe-type dynamics described in [17] may exist. The values of (k, ϵ) considered in this subsection correspond to values of the parameters which lie to the left of the wedge-shaped regions in Figures 6 and 9.

Proposition 4B.1. There exists $N = N(\epsilon, k)$ which becomes unbounded as $\epsilon \to 0$ such that if $0 \leq j \leq N$, then each H^j and G^j consists of a unique curve in $\mathcal{T}'$ and $\mathcal{F}_0$, respectively. These curves can be written as

$$\begin{aligned} H^j &= \{(x, \delta_z, u) \in \mathcal{T}' : u = H^j(x)\}, \\ G^j &= \{(\delta_x, z, u) \in \mathcal{F}_0 : z = G^j(u)\}. \end{aligned} \tag{4B.1}$$

Each $H^j(x)$ and $G^j(u)$ is a nondecreasing function. If $i < j$, then $H^i(x) > H^j(x)$ whenever both of these functions are defined, and $G^i(u) < G^j(u)$ whenever both of these functions are defined.

Remark. Each $H^j(x)$ may not be defined for all $x \in (0, \delta_x)$, and each $G^j(u)$ may not be defined for all $u \in (-\delta_u, \delta_u)$. What is true, however, is that for each $j, 0 \leq j \leq N$, there exist positive constants x_j and u_j such that $H^j(x)$ is defined for $0 \leq x \leq x_j$ and $G^j(u)$ is defined for $-\delta_u \leq u \leq u_j$.

Proof of Proposition 4B.1. In what follows, the reader is referred to Figure 13A. We first consider the case $j = 0$. Since $G^0 = \ell_u$, it follows from (3C.7) that $G^0 = \{(\delta_x, z, u) \in \mathcal{F}_0 : z = 0\}$. We, therefore, set $G^0(u) \equiv 0$. Corollary 3C.2 implies that $H^0 \equiv \psi(G^0) \cap \mathcal{T}'$ is a smooth curve in $\mathcal{T}'$ which can be written as $H^0 = \{(x, \delta_x, u) \in \mathcal{T}' : u = H^0(x)\}$. Here $H^0(x)$ is a smooth increasing function. Recall from (3C.9) that $k < k(\epsilon)$ implies that $H^0(0) < -k$.

Now suppose that for $0 \leq j \leq J$, each H^j and G^j can be written in the form (4B.1) where $H^j(x)$ and $G^j(u)$ are nondecreasing functions. We also assume that if $i < j \leq J$, then $H^i(x) > H^j(x)$ whenever both of these functions are defined and $G^i(u) < G^j(u)$ whenever both of these functions are defined. This implies that if $0 < j \leq J$, then $H^j(0) < H^0(0) < -k$.

We apply Lemma 3B.4 with $\hat{\alpha}$ replaced with H^J to conclude that $\hat{G}^{J+1} = \varphi(H^J)$ can be written as $\hat{G}^{J+1} = \{(\delta_x, z, u) \in \mathcal{F} : z = G^{J+1}(u)\}$. Moreover, $G^{J+1}(u)$ is an increasing function. Since $H^J(x) < H^{J-1}(x)$, it follows from Corollary 3B.3 that $G^J(u) < G^{J+1}(u)$ whenever both functions are defined. It is possible that $\hat{G}^{J+1} \cap \mathcal{F}_0 = \emptyset$; that is, $G^{J+1}(u)$ is only defined for $u < -\frac{1}{2}\delta_u$. In this case we set $N = J$, and the proof is complete. If $\hat{G}^{J+1} \cap \mathcal{F}_0 \neq \emptyset$, then we set $G^{J+1} = \hat{G}^{J+1} \cap \mathcal{F}_0$.

Assume that $\hat{G}^{J+1} \cap \mathcal{F}_0 \neq \emptyset$. Corollary 3C.2, with $\hat{\alpha}$ replaced with G^{J+1}, implies that $H^{J+1} = \psi(G^{J+1}) \cap \mathcal{T}'$ can be written in the form $H^{J+1} = \{(x, \delta_z, u) \in \mathcal{T}' : u = H^{J+1}(x)\}$ where $(H^{J+1})'(x) \geq 0$. Since $G^J(u) < G^1_{J+1}(u)$, we conclude from Remark 3C.3 that $H^{J+1}(x) < H^J(x)$.

It is not hard to prove that there exists a constant C_1, which does not depend on ϵ or k, such that $N(\epsilon, k) > C_1/\epsilon$. This is equivalent to proving that there exists a constant C_0 such that, for each j and x, $|H^j(x) - H^{j-1}(x)| < C_0\epsilon$ and $|G^j(u) - G^{j+1}(u)| < C_0\epsilon$. These estimates are proved inductively; the estimate for the G^js follows from the explicit formula for φ given in (3B.6) while the estimate for the H^js follows from the third equation in (2A.1) together with the fact that the time it takes a trajectory to get from $\mathcal{F}$ to $\mathcal{T}$ is bounded independently of ϵ and k. A more precise statement and proof of the result needed here are given in Lemma 5A.1.

C. The Case: $k = k(\epsilon)$

We briefly discuss the nature of the curves $\{H^j\}$ and $\{G^j\}$ when $k = k(\epsilon)$. Recall, from Proposition 3C.4 that when $k = k(\epsilon)$, (2A.1) gives rise to a homoclinic orbit. We shall see that the qualitative features of the curves $\{H^j\}$ and $\{G^j\}$ are precisely as in the preceding subsection, except for the curve G^1. We do not give a detailed proof of every statement in this subsection, since this subsection is presented mostly for the sake of completeness; the results presented here are not necessary for the description of the dynamics presented later.

As before, $G^0 = \{(\delta_x, z, u) \in \mathcal{F}_0 : z = 0\}$, and, by Corollary 3C.2, $H^0 = \psi(G^0) \cap \mathcal{T}'$ can be written as $H^0 = \{(x, \delta_z, u) \in \mathcal{T}' : u = H^0(x)\}$. Let $p_k = (0, \delta_z, H^0(0))$. Since $k = k(\epsilon)$, it follows that $p_k \in W^u \cap W^s_{loc}$ and $H^0(0) = -k$.

We next consider $G^1 = \varphi(H^0)$. Since $H^0(0) = -k$, this curve is qualitatively similar to the curve shown in Figure 11C. That is, $G^1 = \{(\delta_x, z, u) \in \mathcal{F}_0 : z = G^1(u)\}$ where $G^1(u)$ is a smooth function defined for $u \geq -k$ such that $G^1(-k) = 0$, $(G^1)'(-k) = 0$, and $(G^1)'(u) > 0$ for $u > -k$. Let $q_1 = (\delta_x, 0, -k)$ and $q_2 = \psi(q_1)$. Since $q_1 \in G^0$, it follows that $q_2 \in H^0$.

Suppose that $q_2 = (x_2, \delta_z, u_2)$. In Figure 13B, we have placed q_2 so that $x_2 < 0$. This fact will follow from Lemma 5A.1. Corollary 3C.2 now implies that $H^1 = \psi(G^1) \cap \mathcal{T}'$ can be written as $H^1 = \{(x, \delta_z, u) \in \mathcal{T}' : u = H^1(x)\}$. Here, $H^1(x)$ is defined for $0 \leq x \leq x_0$ for some $x_0 > 0$. Moreover, $H^1(x) < H^0(x)$ for $0 \leq x \leq x_0$.

We now proceed as in the preceding subsection to conclude that there exists N such that if $1 < j \leq N(\epsilon)$, then $\{H^j\}$ and $\{G^j\}$ satsify the conclusions of Proposition 4B.1.

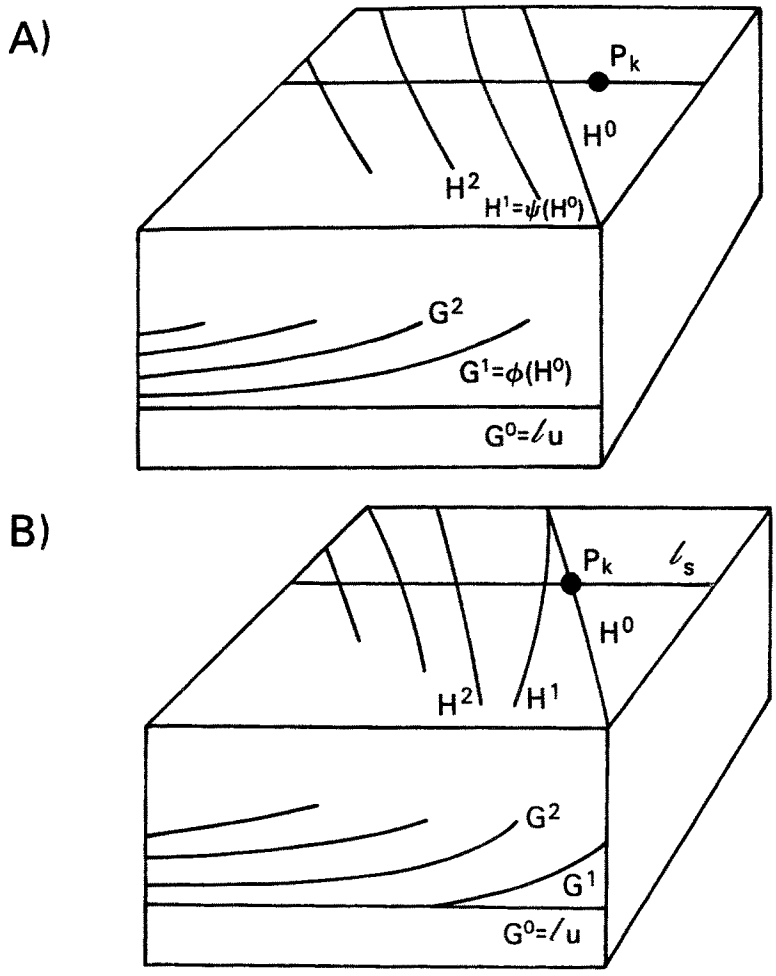

Fig. 13. The curves H^i and G^i for (A) $k < k(\epsilon)$, and (B) $k = k(\epsilon)$. Note that when $k = k(\epsilon)$, the curves H^1 and G^1 end along the curves H^0 and G^0, respectively.

D. The Sector S_1

We now increase k past $k(\epsilon)$ and demonstrate that there exists $k_1(\epsilon) > k(\epsilon)$ such that if $k \in (k(\epsilon), k_1(\epsilon))$, then (2A.1) gives rise to a periodic solution. This range of parameters corresponds to the sector S_1 in Figure 9.

As before, we let $G^0 = \ell_u$ and $H^0 = \psi(G^0) \cap \mathcal{T}' = \{(x, \delta_z, u) \in \mathcal{T}' : u = H^0(x)\}$. We assume that $k > k(\epsilon)$; recall, from (3C.9), that this implies that $H^0(0) > -k$. We also assume that $0 < H^0(0) + k < \epsilon^{(\lambda_2 - \lambda)/\lambda_1}$ where λ is as in (3D.1). We now apply Proposition 3D.1 with $\hat{\alpha} = H^0$. It follows that $\pi(H_0) \cap \mathcal{T}' = H_1 \cup H_2$ where H_1 and H_2 are disjoint curves which can be written as $H_i = \{(x, \delta_z, u) \in$

$\mathcal{T}' : u = H_i(x)\}, i = 1, 2$. Moreover, $H_1(x)$ and $H_2(x)$ satisfy (3D.2) with $\alpha_1(x)$ and $\alpha_2(x)$ replaced with $H_1(x)$ and $H_2(x)$, respectively. Let $H^1 = H_1 \cup H_2$. Recall that each of these curves depends on the parameters ϵ and k.

We conclude from (3D.2f) that

$$H^0(0) - C_3\epsilon^{\lambda_2/\lambda_1} < H_1(0) < H^0(0) - C_4\epsilon^{\lambda_2/\lambda_1}. \tag{4D.1}$$

This implies that if $H^0(0) + k < C_4\epsilon^{\lambda_2/\lambda_1}$, then $H_1(0) + k < 0$. Moreover, if ϵ is sufficiently small and

$$C_3\epsilon^{\lambda_2/\lambda_1} < H^0(0) + k < \epsilon^{(\lambda_2-\lambda)/\lambda_1},$$

then (4D.1) implies that $H_1(0)+k > 0$. Therefore, there must exist $k = k_1(\epsilon) > k(\epsilon)$ such that

$$C_4\epsilon^{\lambda_2/\lambda_1} < H^0(0) + k_1(\epsilon) < C_3\epsilon^{\lambda_2/\lambda_1},$$

and $H_1(0) + k_1(\epsilon) = 0$. Note that when $k = k_1(\epsilon)$, (2A.1) gives rise to a homoclinic orbit. This homoclinic orbit has winding number two in the sense that it intersects both $\mathcal{F}$ and $\mathcal{T}$ twice. It is possible that $k = k_1(\epsilon)$ is not the only solution of the equation $H_1(0) + k_1(\epsilon) = 0$. We assume, however, that the solution of this equation is unique. This is to avoid more notation; the proof of Theorem 2C.1 extends easily to the case when $k_1(\epsilon)$ is not uniquely determined.

We assume throughout the remainder of this subsection that $k(\epsilon) < k < k_1(\epsilon)$. It follows from (3D.2g) that $H_2(0) + k > 0$. Therefore,

$$H^0(0) - C_3\epsilon^{\lambda_2/\lambda_1} < H_1(0) < -k < H_2(0) < H^0(0). \tag{4D.2}$$

Note that (3D.2c) implies that $H_2(x)$ is defined for $0 \le x \le \delta_x$. Let C_0 be as in the statement of Proposition 3D.1. We may assume, without loss of generality, that $C_0 \le \delta_x$. Let

$$\Sigma_0 = \{(x, \delta_z, u) \in \mathcal{T}' : H_2(x) < u < H^0(x), 0 \le x < C_0\}. \tag{4D.3}$$

This is the region which corresponds to the Σ_0 in Section 2B. We claim that $\pi = \pi(\epsilon, k)$ has a fixed point in Σ_0.

To prove that π has a fixed point in Σ_0, we consider $\pi(\Sigma_0) \cap (\Sigma_0)$. Since Σ_0 lies between H^0 and H_2, we first determine $\pi(H^0)$ and $\pi(H_2)$. From the definitions it follows that $\pi(H^0) \cap \Sigma_0 = H_2 \cap \Sigma_0$. This is shown in Figure 14. Moreover, Proposition 3D.1 and (4D.1) imply that $\pi(H_2) \cap \mathcal{T}' = H_{21} \cup H_{22}$ where H_{21} and H_{22} are smooth curves in $\mathcal{T}'$ which can be written as $H_{2i} = \{(x, \delta_z, u) \in \mathcal{T}' : u = H_{2i}(x)\}$, $i = 1, 2$. From the (3D.2c), $H_{22}(x)$ is defined for $0 \le x \le C_0$. Moreover, Corollary 3B.3, Remark 3C.3, (4D.2), and (3D.2g) imply that

$$H_{21}(0) < H_1(0) < H_2(0) < H_{22}(0) < H^0(0). \tag{4D.4}$$

Therefore, $H_2(x) < H_{22}(x) < H^0(x)$ for $0 \le x \le C_0$, and

$$\pi(\Sigma_0) \cap \Sigma_0 = \{(x, \delta_z, u) : H_2(x) < u < H_{22}(x), 0 \le x \le C_0\} \equiv V_{00}. \tag{4D.5}$$

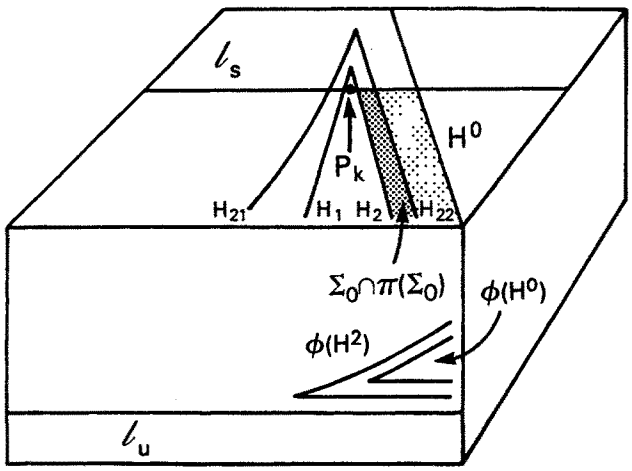

Fig. 14. The case $k(\epsilon) > k_1(\epsilon)$. The set Σ_0 lies between the curves H^0 and H^2. The set $\Sigma_0 \cap \pi(\Sigma_0)$ lies between H_2 and H_{22}.

In order to complete the proof that π contains a hyperbolic, periodic solution we must consider $\pi^{-1}(\Sigma_0)$ and prove that, restricted to $\pi^{-1}(\Sigma_0)$, $D\pi$ satisfies the contraction and expansion conditions given in (h2) and (h3) of Section 2B. This analysis is carried out in Section 5.

E. The Sectors S_2 and S_3

As in the preceeding subsection, we assume that $0 < H^0(0) + k < \epsilon^{(\lambda_2-\lambda)/\lambda_1}$. Let H^0, H_1, H_2, H_{12} and H_{21} be as defined earlier. Recall that $\pi(H_2) \cap \mathcal{T}' = H_{21} \cup H_{22}$. Moreover, each of these curves depends on the parameters ϵ and k. We must now consider $\pi(H_1) \cap \mathcal{T}'$.

From Proposition 2D.1, we conclude that $\pi(H_1) \cap \mathcal{T}' = H_{11} \cup H_{12}$ where H_{11} and H_{12} are smooth curves in $\mathcal{T}$ which can be written as $H_{1i} = \{(x, \delta_z, u) \in \mathcal{T} : u = H_{1i}(x)\}, i = 1, 2$. Using Corollary 3B.3, Remark 3C.3, (4D.4), and the definitions, we conclude that

$$H_{11}(0) < H_{21}(0) < H_1(0) < H_2(0) < H_{22}(0) < H_{12}(0) < H_0(0). \quad \text{(4E.1)}$$

These curves are illustrated in Figure 15. Each curve may not be defined for all $x \in [0, \delta_x]$. However, from (3D.2b), we conclude that each curve is defined for $x \in [0, C_2C_0]$.

Recall that $k_1(\epsilon)$ is such that $H_2(0) = -k_1(\epsilon)$. Analysis similar to that given before demonstrates that there exists $k_2(\epsilon)$ and $k_3(\epsilon)$ such that

$$k_1(\epsilon) < k_2(\epsilon) < k_3(\epsilon), \quad H_{21}(0) = -k_2(\epsilon), \quad H_{11}(0) = -k_3(\epsilon).$$

Moreover, for $i = 2$ or 3, $C_4\epsilon^{\lambda_2/\lambda_1} < H_0(0) + k_i(\epsilon) < C_3\epsilon^{\lambda_2/\lambda_1}$. This last statement follows from (3D.2f). Note that when $k = k_2(\epsilon)$ or $k_3(\epsilon)$, (2A.1) gives rise to a homoclinic orbit of winding number three. As with $k(\epsilon)$ and $k_1(\epsilon)$, we cannot

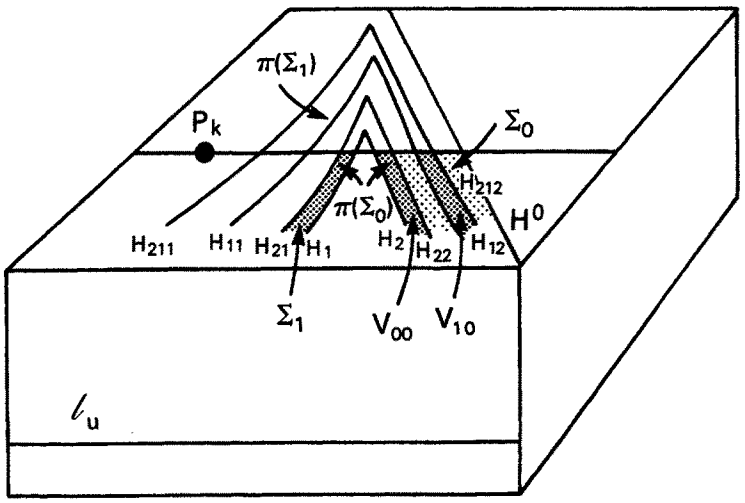

Fig. 15. Here $\pi(\epsilon, k)$ gives rise to Fibonacci dynamics. Note that $\pi(\Sigma_0) \cap \Sigma_0 = V_{00}$ and $\pi(\Sigma_0) \cap \Sigma_1 = \Sigma_1$ are vertical strips in Σ_0 and Σ_1, respectively. Moreover, $\pi(\Sigma_1) \cap \Sigma_0 = V_{01}$ is a vertical strip in Σ_0 and $\pi(\Sigma_1) \cap \Sigma_1 = \emptyset$.

conclude that $k_2(\epsilon)$ and $k_3(\epsilon)$ are the only solutions of the equation $H_{21}(k)(0) = -k$ and $H_{11}(k)(0) = -k$, respectively. We assume that they are uniquely determined; there is no problem in extending the proof in case they are not.

The region $\{(k, \epsilon) : k_1(\epsilon) < k < k_2(\epsilon)\}$ corresponds to the sector S_2 in Figure 9, while the region $\{(k, \epsilon) : k_2(\epsilon) < k < k_3(\epsilon)\}$ corresponds to the sector S_3 in Figure 9. We assume that $k_2(\epsilon) < k < k_3(\epsilon)$ throughout the remainder of this subsection. We demonstrate that for these values of the parameters, (2A.1) gives rise to the Fibonacci dynamics described in Proposition 2B.2.

Let Σ_0 be as in (4D.3), and let

$$\Sigma_1 = \{(x, \delta_z, u) \in \mathcal{T}' : 0 \le x \le C_2C_0, H_{21}(x) < u < H_1(x)\}. \quad (4E.2)$$

We must now study the sets $\pi(\Sigma_i) \cap \Sigma_j$, i and $j = 0, 1$. In (4D.5) we saw that

$$V_{00} \equiv \pi(\Sigma_0) \cap \Sigma_0 = \{(x, \delta_z, u) \in \Sigma_0 : H_2(x) < u < H_{22}\} \subset \Sigma_0.$$

We show later, in Section 5D, that this is a vertical strip in Σ_0. From the definitions it follows that $V_{01} \equiv \pi(\Sigma_0) \cap \Sigma_1 = \Sigma_1$. In particular, V_{01} is a vertical strip in Σ_1.

We must still consider $\pi(\Sigma_1)$. Since Σ_1 lies between the curves H_{21} and H_1, we must study $\pi(H_{21})$. From Proposition 3D.1, it follows that $\pi(H_{21}) \cap \mathcal{T}' = H_{211} \cup H_{212}$ where $H_{21i} = \{(x, \delta_z, u) \in \mathcal{T}' : u = H_{21i}(x)\}$. The function $H_{212}(x)$ is defined for $0 \le x \le \delta_x$. Using Corollary 3B.3 and Remark 3C.3, we conclude that $H_{211}(0) < H_{21}(0)$ and $H_{12}(0) < H_{212}(0) < H^0(0)$. This implies that $\pi(\Sigma_1) \cap \Sigma_1 = \emptyset$, and

$$V_{10} \equiv \pi(\Sigma_1) \cap \Sigma_0 = \{(x, \delta_z, u) : 0 \le x \le C_0, H_{12}(x) < u < H_{212}(x)\}.$$

We demonstrate in Section 5 that V_{10} is a vertical strip in Σ_0.

Let $V = V_{00} \cup V_1 \cup V_{10}$ and $H = \pi^{-1}(V)$. In order to complete the proof that π gives rise to Fibonacci dynamics, we must show that on H, $D\pi$ satisfies the

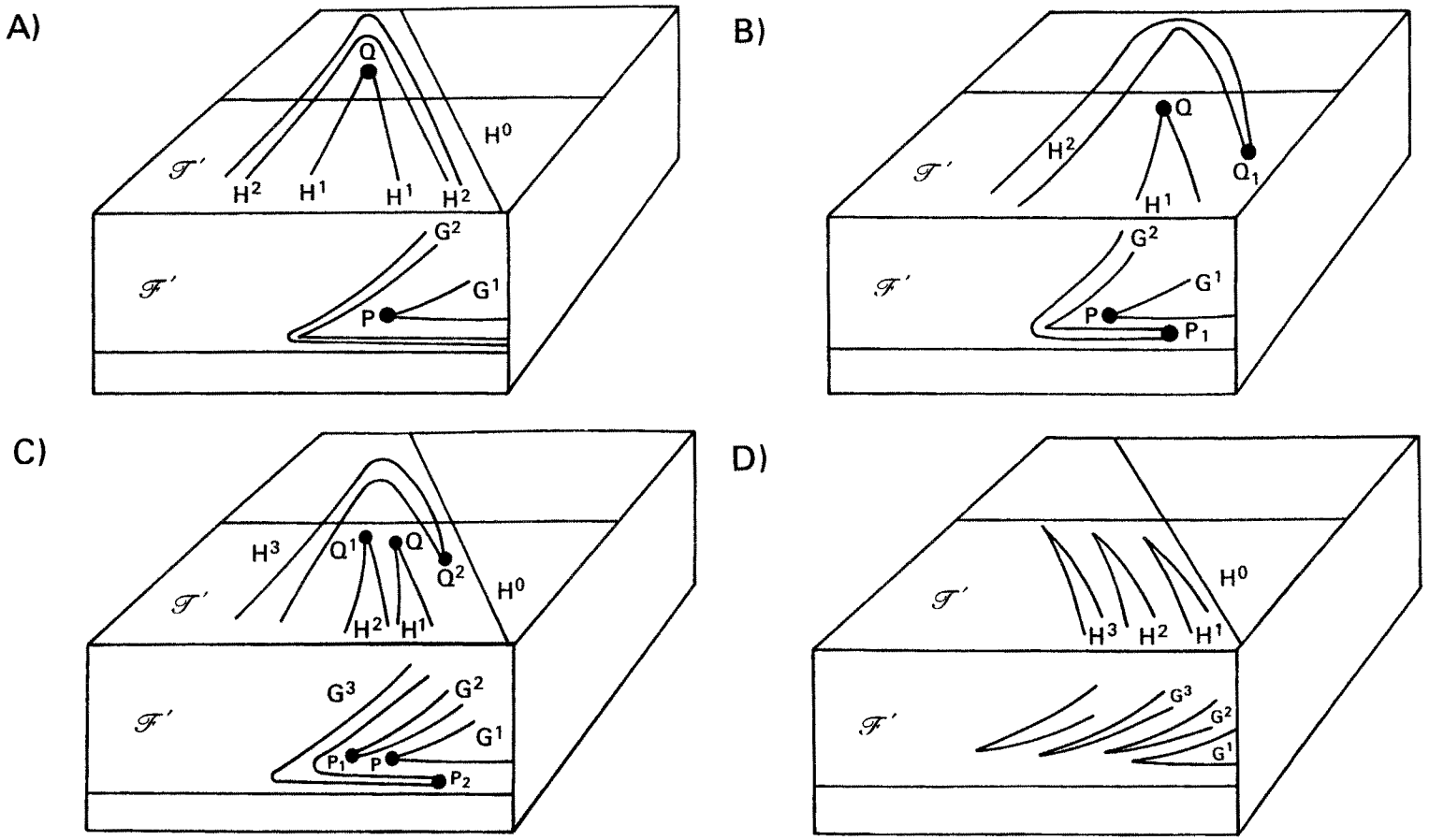

Fig. 16. Transition to continuous spiking. These figures illustrate how the curves H^j and G^j, $j \leq 0$, unwind as k increases. Continuous spiking is achieved when each H^j consists of just one curve which lies in $\mathcal{T}'$. This is illustrated in (D).

contraction and expansion properties described in Section 2B. These properties are verified in Section 5D.

F. The Case: $C_3\epsilon^{\lambda_2/\lambda_1} < H^0(0) + k < \epsilon^{(\lambda_2-\lambda)/\lambda_1}$

As k increases, (2A.1) gives rise to increasingly more complicated dynamics. The sets Σ_j in Figure 8 correspond to components of $\pi^j(\Sigma_0) \cap \mathcal{T}'$, $j \geq 0$. As k increases, the point $p_k = (0, \delta_z, -k) = W^s_{loc} \cap \mathcal{T}$ passes through more and more of these components. As this happens, (2A.1) gives rise to increasingly more complicated Fibonnacci dynamics, as described in Theorem 2C.1. The dynamics is, in some sense, the most interesting when

$$C_3\epsilon^{\lambda_2/\lambda_1} < H^0(0) + k < \epsilon^{(\lambda_2-\lambda)/\lambda_1}. \tag{4F.1}$$

The constants C_3 and λ are as in the statement of Proposition 3D.1. This range of parameters corresponds to the region just to "right" of the sectors $\{S_i\}$ in Figure 9. We now describe the dynamics for this range of parameters. As before, we often drop, in our notation, the dependence of various objects on ϵ and k.

We now describe the iterates $\pi^j(\Sigma_0)$, $j \geq 1$, in order to define the sectors Σ_j that appear in Figure 9. Note that each iterate of Σ_0 must lie between two iterates of H^0. We also recall, from the statement of Proposition 3D.1, that $0 < C_2 < 1$. What follows will help clarify the remark preceding Figure 9 that while there exist infinetly many sectors, each line segment $\epsilon = \epsilon_0$, constant, may only cross finitely many of these sectors.

Let Σ_1 be as in (4E.2). Recall that

$$\Sigma_1 = \{(x, \delta_z, u) \in \mathcal{T}' : 0 \leq x \leq C_2C_0, H_{21}(x) < u < H_1(x)\}.$$

In order to describe $\pi(\Sigma_1)$, we must study $\pi(H_1)$ and $\pi(H_{21})$. These curves were actually considered in the preceding subsection. Proposition 3D.1, together with (4F.1), implies that

$$\pi(H_1) \cap \mathcal{T}' = H_{11} \cup H_{12} \quad \text{and} \quad \pi(H_{21}) \cap \mathcal{T}' = H_{211} \cup H_{212}$$

where each of the curves $H_\beta, \beta \in \{11, 12, 211, 212\}$, can be written in the form $H_\beta = \{(x, \delta_z, u) \in \mathcal{T}' : u = H_\beta(x)\}$. The functions $H_\beta(x)$ satisfy the conclusions of Proposition 3D.1. Moreover,

$$H_{211}(0) < H_{11}(0) < H_{12}(0) < H_{212}(0).$$

This is shown in Figure 15. Since $H_1(x)$ and $H_{21}(x)$ are only defined for $0 \leq x \leq C_2C_0$, we can only conclude from Proposition 3D.1 that the functions $H_{211}(x)$ and $H_{11}(x)$ are "well behaved" (that is, satisfy (3D.2a, b)) for $0 \leq x \leq C_2^2C_0$. Let

$$\Sigma_2 = \{(x, \delta_2, u) \in \mathcal{T}' : 0 \leq x \leq C_2^2C_0, H_{211}(x) < u < H_{11}(x)\}.$$

Note that (4F.1) and (3D.2f) imply that

$$-k < H_0(0) - C_3\epsilon^{\lambda_2/\lambda_1} < H_{211}(0) < H_{11}(0) < H^0(0) - C_4\epsilon^{\lambda_2/\lambda_1},$$

and we apply Proposition 3D.1, once again, to H_{211} and H_{11}.

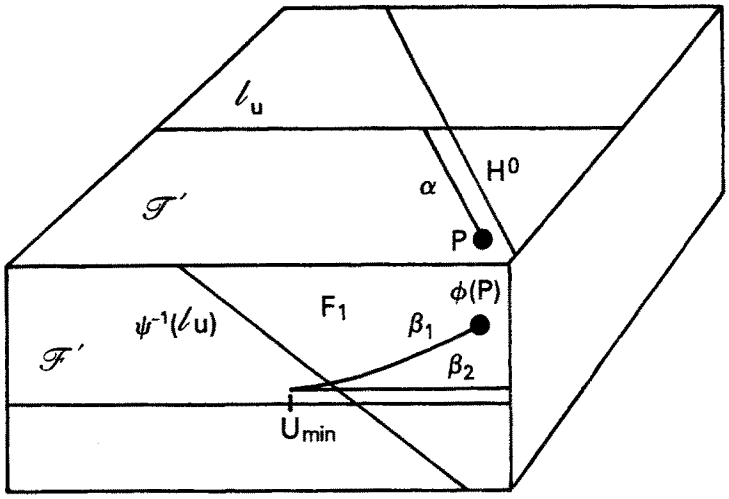

Fig. 17. Objects needed in the proof of Lemma 5B.1. F_1 is the subset of $\mathcal{F}'$ which lies to the right side of the curve $\varphi^{-1}(l_u)$. Note that $\beta = \phi(\alpha)$ intersects F_1 along two disjoint curves. These are denoted by B_1 and B_2.

Now assume that Σ_j, $j \geq 1$, has been defined. We demonstrate how to define Σ_{j+1}. We assume that Σ_j is that of the form

$$\Sigma_j = \{(x, \delta_z, u) \subset \mathcal{T}' : 0 \leq x \leq C_2^j C_0, H_{\alpha_j}(x) < u < H_{\beta_j}(x)\}$$

where $\alpha_j = 211\cdots1$ and $\beta_j = 11\cdots1$. In both α_j and β_j, the number of 1's is j. We assume that for $0 \leq x \leq C_2^j C_0$, the functions $H_{\alpha_j}(x)$ and $H_{\beta_j}(x)$ satisfy the conclusions of Proposition 3D.1. Moreover,

$$\Sigma_j = \pi(\Sigma_{j-1}) \cap \mathcal{T}' \cap (\text{compliment of } \Sigma_1).$$

That is, $\pi(\Sigma_{j-1}) \cap \mathcal{T}'$ consists of two components. One of these is contained in Σ_1. The other component is Σ_j. Finally, we assume that $H_{\alpha_j}(x) < H_{\beta_j}(x) < H_{\alpha_{j-1}}(x)$ for each x for which all of these functions are defined, and

$$-k < H_0(0) = C_3\epsilon^{\lambda_2/\lambda_1} < H_{\alpha_j}(0) < H_{\beta_j}(0) < H^0(0) - C_4\epsilon^{\lambda_2/\lambda_1}.$$

We have already proven that each of these conditions is satisfied if $j = 2$.

We now wish to define Σ_{j+1} and demonstrate that it satisfies each of the conditions described in the preceding paragraph. To do this we must consider $\pi(H_{\alpha_j})$ and $\pi(H_{\beta_j})$. However, since H_{α_j} and H_{β_j} may only be defined for $0 \leq x \leq C_2^j C_0$, we are only able to apply Proposition 3D.1, with $\hat{\alpha}$ replaced with either H_{α_j} or H_{β_j}, if $C_2^j C_0 > \epsilon C_1$. Therefore, we must assume that $j < N = N(\epsilon)$ where

$$N(\epsilon) \leq -\ln\left(\frac{\epsilon C_1}{C_0}\right) / \ln C_2.$$

If $j < N(\epsilon)$, then according to Proposition 3D.1 we have that

$$H_{\alpha_{j+1}} \equiv \pi(H_{\alpha_j}) \cap \mathcal{T}' \cap (\text{compliment of}) \Sigma_1,$$
$$H_{\beta_{j+1}} \equiv \pi(H_{\beta_{j+1}}) \cap \mathcal{T}' \cap (\text{compliment of}) \Sigma_1,$$

are smooth curves which satisfy all of the conditions of the preceding paragraph. We then set

$$\Sigma_{j+1} = \{(x, \delta_z, u) \in \mathcal{T}' : 0 \le x \le C_2^{j+1} C_0, H_{\alpha_{j+1}}(x) < u < H_{\beta_{j+1}}(x)\}.$$

We note that for each $j, 0 \le j \le N(\epsilon) - 1, \pi(\Sigma_j) \cap \mathcal{T}'$ consists of two components, say V_{j+1} and V_{j0} From our construction we have that $V_{j+1} \cap \Sigma_{j+1} = \Sigma_{j+1}$, and V_{j0} is a vertical strip in Σ_0. In Section 5D we consider $D\pi$ and prove that it satisfies the contraction and expansion conditions described in (h2) and (h3). It then follows from the considerations in Section 2B that (2A.1) gives rise to N-Fibonnacci dynamics.

G. Transition to Continuous Spiking

We now briefly discuss how (2A.1) makes the transition from the Fibonacci dynamics described earlier to continuous spiking. We do not give a detailed, rigorous analysis of all of the bifurcations which must take place during this transition, since such a description is beyond the scope of this paper. Our description is in terms of how the unstable manifold of the fixed point q_k intersects the sides, $\mathcal{T}$ and $\mathcal{F}$, of $\mathcal{R}$. In the previous sections we saw that these intersections consist of collections of curves. We increase k and study how the qualitative features of these curves change. This allows us to understand how continuous spiking arises. Of course, we assume throughout this discussion that ϵ is sufficiently small. In what follows we drop the dependence on k in our notation.

We begin where we left off in the previous section; that is, assume that $0 < H^0(k) + k < \epsilon^{(\lambda_2 - \lambda)/\lambda_1}$. This case is illustrated in Figure 16A where we show $H^0 = H^0(k), G^1 = \varphi(H^0)$, and $H^1 = \psi(G^1) = \pi(H^0)$. Note that G^1 can be written as $G^1 = \{(\delta_x, z, u) : u = G^1(z)\}$. The function $G^1(z)$ has a unique minimum at, say, $z = z_0$. Let $P = (\delta_x, z_0, G^1(z_0))$ and $Q = \psi(P)$. We assume that $Q = (x_1, \delta_z, u_1)$. Of course, all of these quantities depend on the parameter k. Recall that since $0 \le H^0 + k \le \epsilon^{(\lambda_2 - \lambda)/\lambda_1}$, $x_1 = x_1(k) < 0$. This is equivalent to the saying that $Q = Q(k) \notin \mathcal{T}'$. This fact was very important in our previous analysis. Because $Q \notin \mathcal{T}'$, we were able to conclude that $H^1 \cap \mathcal{T}'$ is the union of two, disjoint empty curves. These curves were denoted in Section 4D by H_1 and H_2. A key step in understanding how continuous spiking arises is to follow the point $Q(k)$ as k increases. We will see that as k increases, $Q(k)$ must eventually cross ℓ_s into $\mathcal{T}'$. As $Q(k)$ progresses deeper into $\mathcal{T}'$, the Fibonacci dynamics disappear until continuous spiking is achieved.

We now assume that there exists k_* such that $x_1(k_*) = 0$ and $x_1(k) > 0$ for $k > k_*$. We shall not verify this assumption in this paper; however, it follows from proof of Theorem 5.1 in [17]. In what follows the reader is referred to Figure 16. In Figure 16 we illustrate $H^0, G^1, H^1, G^2 = \varphi(H^1)$, and $H^2 = \psi(G^2)$ for different values of k. These figures are meant to illustrate how the complex behavior of the unstable manifold "unwinds" as k increases.

Note that in Figure 16A, $H^1 \cap \mathcal{T}'$ consists of two disjoint curves, while $H^2 \cap \mathcal{T}'$ consists of four disjoint curves. This situation changes as k increases. As the point $Q(k)$ moves further into $\mathcal{T}', P_1(k) = \varphi(Q(k))$ eventually lies in $\mathcal{F}$ and $Q_1(k) =$

$\psi(P_1(k))$ lies in $\mathcal{T}'$. This case is illustrated in Figure 16B. It is now the case that $H^2 \cap \mathcal{T}'$ consists of three disjoint curves instead of four. For larger values of k, the point Q_1 crosses ℓ_s into $\mathcal{T}\backslash\mathcal{T}'$, and then crosses ℓ_s again until Q_1 lies in $\mathcal{T}'$. It is then the case that $H^2 \cap \mathcal{T}'$ consists of just one curve. This is shown in Figure 16C where we also illustrate $G^3 = \varphi(H^2), H^3 = \psi(G^3), P_2 = \varphi(Q_1)$ and $Q_2 = \psi(P_2)$. With increasing k, the point Q_1 moves into $\mathcal{T}'$ and the point P_2 moves into $\mathcal{F}$. As this happens, $Q_2 = \psi(P_2)$ enters $\mathcal{T}'$ as shown in Figure 17C. For larger values of k, Q_2 crosses ℓ_s into $\mathcal{T}\backslash\mathcal{T}'$ and then crosses ℓ_s again so that it is back into $\mathcal{T}'$. In this case, $H^3 \cap \mathcal{T}'$ consists of one curve as shown in Figure 16D.

As k increases, each family of curves H^j "unwinds" as described in the preceding paragraph. Continuous spiking (or, perhaps, "chaotic" continous spiking) is achieved when each set H^j consists of one curve which lies in $\mathcal{T}'$. This is illustrated in Figure 16D. Note that the set of curves $\{H^j\}$ converges to an invariant, two-dimensional manifold which we denote by $\mathcal{P}(\epsilon, k)$ As described in [17, Section 5], continous spiking corresponds to a stable periodic orbit on this invariant two-dimensional manifold. This invariant manifold can be obtained as a perturbation of the manifold $\mathcal{P}$ that is described in (A4) of Section 2. See [7].

Remark 4G. Because $\mathcal{P}(\epsilon, k)$ is an invariant two-dimensional manifold, one can describe the dynamics on $\mathcal{P}$ in terms of a one-dimensional map. This is done by considering a one-dimensional cross-section of $\mathcal{P}$. It is well known that one-dimensional maps (the logistic map, for example) may give rise to "chaotic" behavior. If this is the case for (2A.1), then we refer to such a behavior as chaotic continuous spiking. Computer simulations, see [5] and [1] for example, suggest that (2A.1) undergoes chaotic continuous spiking during the transition from bursting to continuous spiking.

Our analysis demonstrates that even if $\pi(\epsilon, k)$ gives rise to Fibonacci dynamics, then the maximal invariant set of $\pi(\epsilon, k)$ lies very close to an invariant, two-dimensional manifold. Recall that if $\pi(\epsilon, k)$ gives rise to Fibonacci dynamics, then the maximal invariant set of $\pi(\epsilon, k)$ lies in the region Σ_0 that was defined in (4D.3). Each point in Σ_0 lies within a distance of order $\epsilon^{r/\epsilon}$ to the curve H^0. Since H^0 is contained in the unstable manifold $W^u_{q_k}$, it follows that the maximal invariant set of $\pi(\epsilon, k)$ is extremely close to the invariant, two-dimensional manifold $W^u_{q_k}$. In the next section, we compute explicitly the eigenvalues and eigenvectors of the linearized flow near the maximal invariant set of $\pi(\epsilon, k)$. This will further demonstrate that this invariant set is strongly dissipative.

5. Proof of Proposition 3D.1

A. Properties of ψ

The proof of Proposition 3D.1 is broken up into a number of lemmas. It is necessary to understand detailed properties of the maps φ and ψ and then fit them together. The most delicate part of the analysis is concerned with the map φ, since it is the singular part. This map is considered in the next subsection. Here we prove important properties of ψ. We always assume that ϵ is sufficiently small.

Lemma 5A.1. *There exist positive constants* δ_0, N_0, and N_1 *such that if* $0 < \epsilon < \delta_0, |k| < \delta_0, \|(\delta_x, z_1, u_1) - (\delta_x, 0, 0)\| < \delta_0$, *and* $\psi(\delta_x, z_1, u_1) = (x_2, \delta_z, u_2)$, *then* $\epsilon N_0 < u_1 - u_2 < \epsilon N_1$.

Proof. We first consider the case $\epsilon = 0$, and then we perturb ϵ. Let $\gamma_h(t)$ be the homoclinic solution of (2A.1) with $\epsilon = 0$. We assume that $t = 0$ is chosen so that $\gamma_h(0) \in \mathcal{F}$. Recall, from (A6), that $g(\gamma_h(t), 0) < 0$ for all t. Choose T_0 so that $\gamma_h(T_0) = \psi(0, 0)(\gamma_h(0))$. Then

$$N_2 \equiv \int_0^{T_0} g(\gamma_h(t), 0)\, dt < 0.$$

It follows from the continuous dependence of solutions that there exists $\delta_0 > 0$ with the following property: Suppose that $0 < \epsilon < \delta_0, |k| < \delta_0, q = (v_1, w_1, y_1) \in \mathcal{F}$ and $\|q - \gamma_h(0)\| < \delta_0$. Let $\gamma_1(t)$ be the solution of (2A.1) with $\gamma_1(0) = q$, and choose $T_1 > 0$ so that $\gamma_1(T_1) = \psi(\epsilon, k)(q)$. Then

$$-2N_2 < \int_0^{T1} g(\gamma_1(T_1), k)\, dt < -\frac{1}{2}N_2.$$

Suppose that $\gamma_1(T_1) = (v_2, w_2, y_2)$. From the last equation in (2A.1) we have that

$$y_2 - y_1 = \epsilon \int_0^{T_1} g(\gamma_1(t), k)\, dt.$$

Therefore, $(\epsilon/2)N_2 < y_1 - y_2 < 2\epsilon N_2$. The result now follows because the change of variables described in Section 2A can be chosen so that $u = y + \epsilon h(p, k)$, $p = (v, w, y)$, where $|h(p, k)| \to 0$ as $\|p\| \to 0$.

In what follows, we let $\mathcal{F}'$ be as in (3B.5) and $H^0 = \psi(\epsilon, k)(\ell_u)$ be as in Section 4. Recall that $H^0 = \{(x, \delta_z, u) \in \mathcal{T}' : u = H^0(x)\}$.

Lemma 5A.2. *Let* N_0 *be as in Lemma 5A.1. Then there exists* $m_0 > 0$ *such that*

$$\mathcal{F}_1 \equiv \mathcal{F}' \cap \psi(\epsilon, k)^{-1}(\mathcal{T}') \subset \{(\delta_x, z, u) \in \mathcal{F} : u > -m_0 z + H_0(0) + \epsilon N_0, z > 0\}.$$

Proof. Let $q_0 = (0, \delta_z, H^0(0))$ and $p_0 = \psi^{-1}(q_0)$. Then, for each k, $q_0 \to (0, \delta_z, 0)$ and $p_0 \to (\delta_x, 0, 0)$ as $\epsilon \to 0$. This was demonstrated in the proof of Proposition 3C.4. Hence, we can choose ϵ sufficiently small so that $\|p_0 - (\delta_x, 0, 0)\| < \delta_0$ for each $k, |k| < \delta_0$. From Lemma 5A.1 it now follows that if $p_0 = (\delta_x, 0, \rho)$, then

$$\epsilon N_0 < \rho - H^0(0) < \epsilon N_1. \tag{5A.1}$$

Let $\ell_s = W^{cs}_{loc} \cap \mathcal{T}$ be as in (3C.4). Of course, $q_0 \in \ell_s$. It follows from Proposition 3C.1 that $\psi^{-1}(\ell_s)$ is a smooth curve in $\mathcal{F}$ which can be written as

$$\psi^{-1}(\ell_s) = \{(\delta_x, z, u) \in \mathcal{F} : u = G(z)\}.$$

Moreover, there exist constants m_0 and m_1, which do not depend on ϵ or k, such that

$$-m_0 < G'(z) < -m_1. \tag{5A.2}$$

Note that $G(0) = \rho$, and $\psi^{-1}(\mathcal{T}') = \{(\delta_x, z, u) \subset \mathcal{F} : u \geq G(z)\}$. Hence, $\mathcal{F}' \cap \psi^{-1}(\mathcal{T}') = \{(\delta_x, z, u) \in \mathcal{F} : z > 0, y \geq G(z)\}$. The result now follows from (5A.1) and (5A.2).

Corollary 5A.3. $\{(\delta_x, z, u) : z > 0, H^0(0) + \epsilon N_1 < u < \frac{1}{2}\delta_u\} \subset \mathcal{F}_1$.

Proof. This follows immediately from the proof of the preceding lemma; see (5A.1) and (5A.2).

B. Properties of φ

We assume throughout this section that the hypotheses of Proposition 3D.1 are satisfied. We always assume that ϵ is sufficiently small. We first prove the proposition in the case when $\alpha(x)$ is of the form $\alpha(x) = \sigma x + b$. Here, $m/2 < \sigma < 2m$ and $-k < b < H(\epsilon, k)(0) = H^0(0)$. After we prove the proposition in this case, the general case will follow easily. In this subsection we prove important properties of $\varphi(\alpha)$.

Lemma 5B.1. *Assume that $\alpha(x) = \sigma x + b$ where $m/2 < \sigma < 2m$ and $-k < b < H^0(0)$. Let $\alpha = \{(x, \delta_z, u) \in \mathcal{T}' : u = \alpha(x)\}$. Then $\varphi(\alpha) \cap \mathcal{F}_1$ is the union of two disjoint, nonempty smooth curves.*

Proof It follows from (3B.7) that $\beta = \varphi(\alpha) \cap \mathcal{F}$ is of the form $\beta = \{(\delta_x, z, u) \in \mathcal{F} : u = \beta(z)\}$ where

$$\beta(z) = -k + \frac{\delta_x}{\sigma}\frac{z}{(\delta_z)}^{(\lambda_1-\epsilon)/\lambda_2} + (b + k)\left(\frac{z}{\delta_z}\right)^{-\epsilon/\lambda_2}. \tag{5B.1}$$

Note that $\beta(z)$ has a minimum at $(z_{\min}, u_{\min})$ where

$$u_{\min} = -k + (b + k)\left[\frac{\epsilon(b + k)}{\delta_x(\lambda_1 - \epsilon)}\right]^{-\epsilon/\lambda_1} + \frac{\delta_x}{\sigma}\left[\frac{\epsilon(b + k)}{\delta_x(\lambda_1 - \epsilon)}\right]^{(\lambda_1-\epsilon)/\lambda_1},$$

$$z_{\min} = \delta_z\left[\frac{\epsilon(b + k)}{(\lambda_1 - \epsilon)\delta_x}\right]^{\lambda_2/\lambda_1}. \tag{5B.2}$$

If $z < z_{\min}$, then $\beta'(z) < 0$, while if $z > z_{\min}$, then $\beta'(z) > 0$. Hence, $\beta = \beta_1 \cup \beta_2$ where $\beta_1 = \beta \cap \{z > z_{\min}\}$ and $\beta_2 = \beta \cap \{z < z_{\min}\}$. We may express each $\beta_i, i = 1, 2$, as $\beta_i = \{(\delta_x, z, u) \in \mathcal{F} : z = \beta_i(u)\}$. To complete the proof of the lemma, we shall demonstrate that $\beta_i \cap \mathcal{F}_1 \neq \emptyset, i = 1, 2$, and $(\delta_x, z_{\min}, u_{\min}) \notin \mathcal{F}_1$.

We first prove that $(\delta_x, z_{\min}, u_{\min}) \notin \mathcal{F}_1$. Recall from the hypothesis of Proposition 3D.1 that $0 < k + H^0(0) < \epsilon^{(\lambda_2-\lambda)/\lambda_1}$. Since $-k < b < H^0(0)$ it follows that

$$0 < k + b < \epsilon^{(\lambda_2-\lambda)/\lambda_1}. \tag{5B.3}$$

From (5B.2) we conclude that there exists $C^0 > 0$, which does not depend on ϵ, such that

$$0 < u_{\min} + k < C^0\epsilon^{(\lambda_2-\lambda)/\lambda_1} \quad \text{and} \quad 0 < z_{\min} < C^0\epsilon^{\lambda_2/\lambda_1}. \tag{5B.4}$$

Therefore, if ϵ is sufficiently small, and m_0 and N_0 are as in Lemma 5A.2, then

$$\begin{aligned} u_{\min} - H^0(0) &= u_{\min} + k - (k + H^0(0)) \\ &< (C^0 + 1)\epsilon^{(\lambda_2 - \lambda)/\lambda_1} \\ &< -m_0 z_{\min} + \epsilon N_0. \end{aligned}$$

It now follows from Lemma 5A.2 that $(\delta_x, z_{\min}, u_{\min}) \notin \mathcal{F}_1$.

We next prove that $\beta_2 \cap \mathcal{F}_1 \neq \emptyset$. From (5B.1) it follows that $\lim_{z \to 0} \beta(z) = \infty$. Hence, $\beta_2(u)$ is defined for all $u \in (u_{\min}, \delta_u)$. Together with Lemma 5A.2, this implies that β_2 must intersect $\mathcal{F}_1$. See Figure 17.

Finally, we prove that $\beta_1 \cap \mathcal{F}_1 \neq \emptyset$. Here we use the assumption in Proposition 3D.1 that $\alpha(x)$ is defined for $0 < x \leq \epsilon C_1$ where C_1 is to be determined. We demonstrate that if C_1 is sufficiently large, ϵ is sufficiently small, $\epsilon C_1 < C < \delta_x$, and $p = (C, \delta_z, \alpha(C))$, then $\varphi(p) \in \mathcal{F}_1 \cap \beta_1$.

Let $p = (C, \delta_x, \alpha(C))$ and $\varphi(p) = (\delta_x, z_1, u_1)$. From (3B.6) we conclude that

$$z_1 = \delta_z \left(\frac{C}{\delta_x}\right)^{\lambda_2/\lambda_1} \quad \text{and} \quad u_1 = -k + (\alpha(C) + k)\left(\frac{\delta_x}{C}\right)^{\epsilon/\lambda_1}. \tag{5B.5}$$

The assumptions of Proposition 3D.1 now imply that if C_1 is sufficiently large, ϵ is sufficiently small, and $C > \epsilon C_1$, then

$$\begin{aligned} u_1 &> \frac{1}{2}\alpha(C) > \frac{\epsilon}{2}\sigma C_1 + b \\ &> -k + \frac{\epsilon}{2}\sigma C_1 \\ &= -(k + H^0(0)) + H^0(0) + \frac{\epsilon}{2}\sigma C_1 \\ &> -\epsilon^{(\lambda_2 - \lambda)/\lambda_1} + H^0(0) + \frac{\epsilon}{2}\sigma C_1 \\ &> H^0(0) + \epsilon N_1. \end{aligned}$$

Together with Corollary 5A.3, this implies that $\varphi(p) \in \mathcal{F}_1$. The reason that $\varphi(0) \in \beta_1$ is that (5B.4) and (5B.5) imply that if C_1 is sufficiently large, then $z_1 > z_{\min}$.

Lemma 5B.2. *Let β_1 and β_2 be as in the preceding lemma and $\hat{\beta}_i = \beta_i \cap \mathcal{F}_1$, $i = 1, 2$. Let $r = [(\lambda_2 - \lambda_1 - 2\lambda)/\lambda_1)]\lambda_2$ be as in (3D.1). Then*

a. if $(\delta_x, z, u) \in \hat{\beta}_1 \cup \hat{\beta}_2$, then $u > -k + \epsilon N_0/2$,

b. $$\frac{1}{2}\delta_z \left(\frac{\sigma(u+k)}{2\delta_x}\right)^{\lambda_2/(\lambda_1 - \epsilon)} \leq \beta_1(u) \leq 2\delta_z \left(\frac{\sigma(u+k)}{\delta_x}\right)^{\lambda_2/(\lambda_1 - \epsilon)} \text{ on } \hat{\beta}_1,$$

c. $$0 \leq \beta_2(u) \leq 2\delta_z \left(\frac{b+k}{u+k}\right)^{\lambda_2/\epsilon} \leq 2\delta_z \epsilon^{r/\epsilon} \text{ on } \hat{\beta}_2. \tag{5B.6}$$

Proof. We write (5B.1) as $\beta(z) = -k + \beta_A(t) + \beta_B(t)$ where

$$\beta_A(z) = \frac{\delta_x}{\sigma}\left(\frac{z}{\delta_z}\right)^{(\lambda_1-\epsilon)/\lambda_2} \quad \text{and} \quad \beta_B(z) = (b+k)\left(\frac{z}{\delta_z}\right)^{-\epsilon/\lambda_2} \tag{5B.7}$$

Let $z_1 = \delta_z[\sigma(y+k)/\delta_x]^{\lambda_2/(\lambda_1-\epsilon)}$. Then $\beta_A(z_1) = y + k$ and $|\beta_B(z_1)| \leq 2\epsilon^{(\lambda_2-\lambda)/\lambda_1}$. It easily follows that $\beta_1(u) \to z_1$ as $\epsilon \to 0$. In particular, if ϵ is sufficiently small, then (5B.6b) holds.

We next prove (5B.6a). Suppose that $u = -k + \epsilon N_0/2$, Using (5B.6b) we have that for some constant C_0, independent of ϵ,

$$0 < \beta_2(u) < \beta_1(u) \leq 2\delta_z\left(\frac{\epsilon\sigma N_0}{\delta_x}\right)^{\lambda_2/(\lambda_1-\epsilon)} < C^0\epsilon^{\lambda_2/(\lambda_1-\epsilon)}.$$

Moreover, for ϵ sufficiently small,

$$\begin{aligned} u - H^0(0) &= u + k - (k + H^0(0)) \\ &< \frac{\epsilon N_0}{2} + \epsilon^{(\lambda_2-\lambda)/\lambda_1} \\ &< \epsilon N_0. \end{aligned}$$

It now follows from Lemma 5A.2 that if $u = -k + \epsilon N_0/2$, then

$$(\delta_x, \beta_1(u), u) \notin \mathcal{F}_1 \quad \text{and} \quad (\delta_x, \beta_2(u), u) \notin \mathcal{F}_1.$$

From this (5B.6c) easily follows.

Finally, we prove (5B.6c). Let $z_2 = \delta_z[(b+k)/(y+k)]^{\lambda_2/\epsilon}$. Then $\beta_B(z_2) = y+k$, while $|\beta_A(z_2)| \leq (\delta_z/\sigma)\epsilon^{(\lambda_2-\lambda_1-3\lambda)/\epsilon}$ for ϵ sufficiently small. Using (5B.6a) it follows that if ϵ is sufficiently small, then

$$z_2 \leq \delta_z\left(\frac{2\epsilon^{(\lambda_2-\lambda)/\epsilon}}{\epsilon N_0}\right) \leq \delta_z\epsilon^{r/\epsilon}.$$

From this, (5B.6c) follows.

Lemma 5B.3. *Suppose that* $\varphi(x, \delta_z, u) = (\delta_x, z_1, u_1) \in \hat{\beta}_1$. *Then* $|u - u_1| \to 0$ *as* $\epsilon \to 0$.

Proof. Recall, from (3B.6), that $z_1 = \delta_z(x/\delta_x)^{\lambda_2/\lambda_1}$ and $x = \delta_x(z/\delta_z)^{\lambda_1/\lambda_2}$. From (5B.6), it follows that for some constants K_1 and K_2,

$$x \geq K_1(u+k)^{\lambda_1/(\lambda_1-\epsilon)} \geq K_2\epsilon^{\lambda_1/(\lambda_1-\epsilon)}. \tag{5B.8}$$

Now (3B.6) also implies that $u_1 = -k + (u+k)(\delta_x/x)^{\epsilon/\lambda_1}$. Together with (5B.8), this implies the desired result.

Remark. The preceding lemma is not true if $\hat{\beta}_1$ is replaced with $\hat{\beta}_2$.

We now estimate $\beta_1'(u)$ and $\beta_2'(u)$. Recall from the statement of Proposition 3D.1 that we only assume that $\alpha(x)$ is defined for $0 \le x \le C$ where $\epsilon C_1 \le C \le C_0$. The constant C_1 was defined in the proof of Lemma 5B.1. In the next lemma we show how to define C_0 and explain why it is necessary. For $C_0 > 0$, to be determined, let $T_* = \{(x, \delta_z, u) \in \mathcal{T} : 0 \le x \le C_0\}$. Let $\beta_1^0 = \hat{\beta}_1 \cap \varphi(\mathcal{T}_*)$ and $\beta_2^0 = \hat{\beta}_2 \cap \varphi(\mathcal{T}_*)$.

Lemma 5B.4. *Let $\alpha(x) = \sigma x + b$ be as before. For each $\delta > 0$ we can choose C_0 such that if ϵ is sufficiently small, then $|\beta_1'(u)| < \delta$ for $(\delta_x, z, u) \in \beta_1^0$, and $|\beta_2'(u)| < \delta$ for $(\delta_x, z, u) \in \beta_2^0$.*

Remark. (a) For each $C_0 > 0$ we can choose ϵ sufficiently small such that $\epsilon C_1 < C_0$. If this is the case, then the proof of Lemma 5B.1 demonstrates that $\hat{\beta}_i \cap \varphi(\mathcal{T}_*) \neq \emptyset$, $i = 1, 2$.

(b) It is necessary to introduce C_0 because it may not be true that $|\beta_1'(u)| < \delta$ for $(\delta_z, \beta_1(u), u) \in \beta_1 \backslash \beta_1^0$.

Proof of Lemma 5B.4. From (5B.1) we have that

$$\beta'(z) = \left(\frac{\lambda_1 - \epsilon}{\lambda_2 \delta_z}\right)\left(\frac{\delta_x}{\sigma}\right)\left(\frac{z}{\delta_z}\right)^{(\lambda_1 - \lambda_2 - \epsilon)/\lambda_2} - \frac{\epsilon(b+k)}{\lambda_2 \delta_z}\left(\frac{z}{\delta_z}\right)^{(-\lambda_2 - \epsilon)/\lambda_2}. \quad (5B.9)$$

Suppose that $(\delta_x, z, u) \in \beta_2^0$. Using (5B.6) and (5B.8) we find that for constants K_i, which do not depend on ϵ, and ϵ small,

$$\begin{aligned}
\beta'(z) &= \left[\frac{z}{\delta_z}\right]^{(-\lambda_2+\epsilon)/\lambda_2}\left[\left(\frac{\lambda_1 - \epsilon}{\lambda_2 \delta_z}\right)\left(\frac{\delta_x}{\sigma}\right)\left(\frac{z}{\delta_z}\right)^{\lambda_1/\lambda_2} - \frac{\epsilon(b+k)}{\lambda_2 \delta_z}\right] \\
&\le \left[2\left(\frac{b+k}{u+k}\right)\right]^{(-\lambda_2+\epsilon)/\epsilon}\left[\left(\frac{\lambda_1 - \epsilon}{\lambda_2 \delta_z}\right)\left(\frac{\delta_x}{\sigma}\right)2^{\lambda_1/\lambda_2}\left(\frac{b+k}{u+k}\right)^{\lambda_1/\epsilon} - \frac{\epsilon(b+k)}{\lambda_2 \delta_z}\right] \\
&\le -K_1 \epsilon (b+k)^{-\lambda_2/\epsilon}(u+k)^{(\lambda_2+\epsilon)/\epsilon} \\
&\le -K_1 \epsilon (H^0(0)+k)^{-\lambda_2/\epsilon}(\epsilon N_0)^{(\lambda_2+\epsilon)/\epsilon} \\
&\le -K_2 \epsilon^{(\lambda_2+2\epsilon)/\epsilon}\epsilon^{[-\lambda_2(\lambda_2-\lambda)]/\lambda_1} \\
&\to -\infty \text{ as } \epsilon \to 0.
\end{aligned}$$

Therefore, if $(\delta_x, z, u) \in \beta_2^0$, then we can make $|\beta_2'(u)| = |(\beta'(z))^{-1}|$ as small as we please by choosing ϵ small.

Now suppose that $p = (\delta_x, z, u) \in \beta_1^0$, and let $q = (x_1, \delta_z, u_1) = \varphi^{-1}(p)$. From Lemma 5B.3, we have that $|u - u_1| \to 0$ as $\epsilon \to 0$. It therefore follows that if $0 \le x_1 \le C_0$ and ϵ is sufficiently small, then

$$\begin{aligned}
|u+k| &\le |u - u_1| + |u_1 + k| \\
&\le |u - u_1| + |\sigma x_1 + b + k| \\
&\le \sigma C_0 + |u - u_1| + |b + k| \\
&\le 2\sigma C_0.
\end{aligned}$$

Therefore, for constants K_i which do not depend on ϵ,

$$\begin{aligned}\beta'(z) &= \left(\frac{z}{\delta_z}\right)^{(\lambda_1-\lambda_2-\epsilon)/\lambda_2}\left[\left(\frac{\lambda_1-\epsilon}{\lambda_1\delta_2}\right)\left(\frac{\delta_x}{\sigma}\right)-\frac{\epsilon(b+k)}{\lambda_2\delta_z}\left(\frac{z}{\delta_z}\right)^{-\lambda_1/\lambda_2}\right]\\ &\geq K_1(u+k)^{(\lambda_1-\lambda_2-\epsilon)/\lambda_1-\epsilon}\left[K_2-K_3\epsilon(b+k)(u+k)^{-\lambda_2/(\lambda_1-\epsilon)}\right]\\ &\geq K_4(u+k)^{(\lambda_1-\lambda_2)/\lambda_1}\left[K_2-K_3\epsilon(H^0(0)+k)(u+k)^{-\lambda_2/(\lambda_1-\epsilon)}\right]\\ &\geq K_0(u+k)^{(\lambda_1-\lambda_2)/\lambda_1}\\ &\geq 2\sigma K_0 C_0^{(\lambda_1-\lambda_2)/\lambda_1}.\end{aligned}$$

We now conclude that $\beta'(z)$ is as large as we please by choosing C_0 small; the choice of C_0 does not depend on ϵ. On β_1^0, $\beta_1'(u) = [\beta'(z)]^{-1}$. This, therefore, completes the proof.

Remark 5B.5 For each result in this section, we assumed that near the homonclinic point q_0, (2A.1) can be written in the simple form (3B.3). Since (3B.3) is linear, we were able to compute $\varphi(\epsilon, k)$ explicitly, and the results of this section were proved using the explicit expression for φ. These results extend, in a straightforward way, to the full system (3B.2) using the variation of constants formula.

C. Completion of the Proof of Proposition 3D.1

We now completes the proof of Proposition 3D.1. For the moment we continue to assume that $\alpha(x)$ is of the form $\alpha(x) = \sigma x + b$. It then follows from Lemma 5B.1 that $\pi(\alpha) \cap \mathcal{T}' = \psi(\varphi(\alpha) \cap \mathcal{F}_1)$ is the union of two disjoint, nonempty curves in $\mathcal{T}'$. Let $\alpha_i = \psi(\hat{\beta}_i)$. From Lemma 5B.4 and Proposition 3C.1, we conclude that each α_i can be expressed as $\alpha_i = \{(x, \delta_z, u) \in \mathcal{T}' : u = \alpha_i(x)\}$. Recall, from the proof of Lemma 5B.1, that $\beta_2(u)$ is defined for each $u \in (u_{\min}, \delta_u)$. The function $\beta_1(u)$ is not, however, defined for each $u \in (u_{\min}, \delta_u)$. Lemma 5B.3 implies that $\beta_1(u)$ is defined for $u \in (u_{\min}, \hat{u})$ where $\hat{u} \to C_0$ as $\epsilon \to 0$.

Lemma 5B.4 and Proposition 3C.1 imply that the functions $\alpha_i(x)$, $i = 1, 2$, satisfy $m/2 < \alpha_i'(x) < 2m$ for each x for which $\alpha_i(x)$ is defined. From Proposition 3C.1 we now conclude that there exists $C_2 \in (0, 1)$ such that $\alpha_1(x)$ is defined for $x \in [0, C_2C_0)$. Since $0 < \beta_1(u) < \beta_2(u)$, it follows from Remark 3C.3 that $\alpha_1(x) < \alpha_2(x) < H^0(x)$ for $0 \leq x < C_0C$. Finally, Proposition 3C.1 and Lemma 5B.2 imply that (3D.2f) and (3D.2g) hold.

This completes the proof of Proposition 3D.1 in the case when $\alpha(x)$ is linear. Now suppose that $\alpha(x)$ is any function which satisfies the hypothesis of Proposition 3D.1. It then follows that $\underline{\alpha}(x) \leq \alpha(x) \leq \bar{\alpha}(x)$ for $0 \leq x \leq C_0$ where $\underline{\alpha}(x) = (m/2x) + \alpha(0)$ and $\bar{\alpha}(x) = 2mx + \alpha(0)$. Let

$$\underline{\alpha} = \{(x, \delta_z, \underline{\alpha}(x)) : 0 \leq x \leq C_0\} \quad \text{and} \quad \bar{\alpha} = \{(x, \delta_z, \bar{\alpha}(x)) : 0 \leq x \leq C_0\}.$$

Since α lies in the subset of $\mathcal{T}'$ bounded by $\underline{\alpha}$ and $\bar{\alpha}$, Corollary 3B.3 and Remark 3C.3 imply that $\pi(\alpha) \cap \mathcal{T}'$ lies in the subset of $\mathcal{T}'$ bounded by $\pi(\underline{\alpha}) \cap \mathcal{T}'$ and $\pi(\bar{\alpha}) \cap \mathcal{T}'$.

Since Proposition 3D.1 applies to both $\underline{\alpha}$ and $\bar{\alpha}$, it follows that this region consists of two components. It then easily follows that $\pi(\alpha) \cap \mathcal{T}'$ is the union of two disjoint curves which satisfy (3D.2 a, c, e, f, g).

To prove (3D.2b) and (3D.2d) we consider the linearized map $D\pi$. The desired estimates are then easily obtained using Proposition 3C.1 and Lemma 5B.2. The map $D\pi$ is computed more explicitly in the next section.

D. Hyperbolic Structure

We now demonstrate that the maximal invariant act of $\pi(\epsilon, k)$ is hyperbolic. Our calculations verify that π satisfies the conditions (h2) and (h3) that are described in Section 2B. Together with the discussion in Section 4, this will complete the proof of Theorem 2C.1.

We verify (h2) and (h3) by computing the eigenvalues and corresponding eigenvectors of the linearized map $D\pi = D\psi \circ D\varphi$. The properties which we need concerning $D\psi$ are stated in Proposition 3C.1, while the properties which we need concerning $D\varphi$ will follow from the explicit formula for φ given in (3B.6).

We assume throughout this section that ϵ is sufficiently small and $0 < H^0(0) + k < \epsilon^{(\lambda_2 - \lambda)/\lambda_1}$. Recall, from Proposition 3D.1, that it is for these values of the parameters that we expect the Fibonacci dynamics to arise.

Let $\Sigma = \{(x, \delta_z, u) \subset \mathcal{T}' : -k + (m/2)x \le u \le H^0(x)\}$. Our discussion in Section 4 demonstrates that the interesting dynamics takes place for π restricted to Σ; that is, if Λ is the maximal invariant set of π, then $\Lambda \subset \Sigma$. Let $B = \varphi(\Sigma) \cap \psi^{-1}(\Sigma)$. It follows from Lemma 5B.2 that $B \subset B_1 \cup B_2$ where

$$B_1 = \left\{ (\delta_x, z, u) \in \mathcal{F} : u > k + \frac{\epsilon N_0}{2}, \frac{1}{2}\delta_z \left(\frac{m(u+k)}{2\delta_x}\right)^{\lambda_2/(\lambda_1 - \epsilon)} \right.$$
$$\left. \le z \le 2\delta_z \left(\frac{2m(u+k)}{\delta_x}\right)^{\lambda_2/(\lambda_1 - \epsilon)} \right\},$$
$$B_2 = \left\{ (\delta_x, z, u) \in \mathcal{F} : u > -k + \frac{\epsilon N_0}{2}, 0 \le z \le 2\delta_z \epsilon^{r/\epsilon} \right\}. \tag{5D.1}$$

Let $H_1 = \varphi^{-1}(B_1)$ and $H_2 = \varphi^{-1}(B_2)$.

Let $p = (x_0, \delta_x, u_0) \in \Sigma$, and let $q = \varphi(p) = (\delta_x, z_1, u_1)$. From (3B.6) it follows that

$$z_1 = \varphi_z(x_0, u_0) = \delta_z \left(\frac{x_0}{\delta_x}\right)^{\lambda_2/\lambda_1} \quad \text{and} \quad u_1 = u(x_0, u_0) = -k + (u_0 + k)\left(\frac{\delta_x}{x_0}\right)^{\epsilon/\lambda_1}. \tag{5D.2}$$

Therefore,

$$D\varphi(p) = \begin{bmatrix} \dfrac{\partial \varphi_z}{\partial x} & \dfrac{\partial \varphi_z}{\partial u} \\ \dfrac{\partial \varphi_u}{\partial x} & \dfrac{\partial \varphi_u}{\partial u} \end{bmatrix} (x_0, u_0)$$

$$= \begin{bmatrix} \dfrac{\delta_z}{\delta_x}\dfrac{\lambda_2}{\lambda_1}\left(\dfrac{x_0}{\delta_x}\right)^{(\lambda_1-\lambda_1)/\lambda_1} & 0 \\ -\dfrac{\epsilon}{\lambda_1\delta_x}(u_0+k)\left(\dfrac{x_0}{\delta_x}\right)^{(-\lambda_1+\epsilon)/\lambda_1} & \left(\dfrac{x_0}{\delta_x}\right)^{-\epsilon/\lambda_1} \end{bmatrix}$$

$$= \begin{bmatrix} K_1 x_0^{(\lambda_2-\lambda_1)/\lambda_1} & 0 \\ -K_2\epsilon(u_1+k)x_0^{-1} & K_3 x_0^{-\epsilon/\lambda_1} \end{bmatrix} \tag{5D.3}$$

where K_1, K_2, and K_3 are positive constants which do not depend on ϵ or k.

According to Proposition 3C.1, $D\psi$ is a regular perturbation of the matrix

$$M = \begin{bmatrix} \beta & \dfrac{1}{m} \\ 0 & 1 \end{bmatrix} \tag{5D.4}$$

We prove the desired estimates for the case when $D\psi = M$. The proof for the more general case is then straightforward. Therefore, assume that

$$D\pi(p) = \begin{bmatrix} A & B \\ C & D \end{bmatrix} \tag{5D.5}$$

where

$$A = \beta K_1 X_0^{(\lambda_2-\lambda_1)/\lambda_1} - \frac{1}{m}K_2\epsilon(u_1+k)x_0^{-1}$$

$$B = \frac{1}{m}K_3 x_0^{-\epsilon/\lambda_1}$$

$$C = -\beta K_2\epsilon(u_1+k)x_0^{-1}$$

$$D = K_3 x_0^{-\epsilon/(\lambda-1)}$$

Now assume that $p \in H_2$ or, equivalently, $q = \varphi(p) \in B_2$.

It follows from (5D.1) that $u_1 > -k + (\epsilon N_0/2)$ and $0 \le z_1 \le 2\delta_z\epsilon^{r/\epsilon} \le 2\delta_z\epsilon^{r/\epsilon}$ where $r = [(\lambda_2 - \lambda_1 - 2\lambda)/\lambda_1]\lambda_2$ is as in (3D.1). Together with (5D.2) this implies that

$$x_0 = \delta_x\left(\frac{z_1}{\delta_x}\right)^{\lambda_1/\lambda_2} \le \delta_x 2^{\lambda_1/\lambda_2}\epsilon^{(\lambda_2-\lambda_1-2\lambda)/\epsilon} \le \epsilon^{(\lambda_2-\lambda_1-3\lambda)/\epsilon} \tag{5D.6}$$

and

$$\epsilon(u_1+k)x_0^{-1+(\epsilon/\lambda_1)} \ge \epsilon^{[(\lambda_2-\lambda_1-4\lambda)/\epsilon]} \tag{5D.7}$$

for ϵ sufficiently small.

We now wish to compute the eigenvalues and eigenvectors of $D\pi(p)$ and determine their behavior as $\epsilon \to 0$. Note that (5D.4) implies that each term in $D\pi(p)$ becomes unbounded as $\epsilon \to 0$ except for the term $\beta K_1 x_0^{(\lambda_2-\lambda_1)/\lambda}$ in A. This term $\to 0$ as $\epsilon \to 0$. Therefore, in order to determine the asympotic behavior of $D\pi(p)$, we may ignore the term $\beta K_1 x_0^{(\lambda_2-\lambda_1)/\lambda}$ and consider the matrix

$$M_1 = x_0^{-\epsilon/\lambda_1} M_0$$

where

$$M_0 = \begin{bmatrix} -\frac{1}{m}K_2\epsilon(u_1+k)x_0^{-1+\epsilon/\lambda_1} & \frac{1}{m}K_3 \\ -\beta K_2\epsilon(u_1+k)x_0^{-1+\epsilon/\lambda_1} & K_3 \end{bmatrix}.$$

The eigenvalues of M_0 are

$$\lambda^{\pm} = \frac{-\text{Trace } M_0 \pm \sqrt{(\text{Trace } M_0)^2 - 4 \det M_0}}{2}$$

$$= \frac{-\text{Trace } M_0 \pm \text{Trace } M_0 \sqrt{1 - [4 \det M_0/(\text{Trace } M_0)^2]}}{2}$$

Now, using (5D.7), we have that

$$\frac{\det M_0}{\text{Trace } M_0} = \frac{(1/m)K_2K_3(\beta-1)\epsilon(u_1+k)x_0^{-1+\epsilon/\lambda_1}}{K_3 - (1/m)K_2\epsilon(u_1+h)x_0^{-1+\epsilon/\lambda_1}}$$

$$\to K_3(\beta-1) \text{ as } \epsilon \to 0$$

and $\det M_0/(\text{Trace } M_0)^2 \to 0$ and $\epsilon \to 0$. Therefore,

$$\text{Trace } M_0 \sqrt{1 - \frac{4 \det M_0}{(\text{Trace } M_0)^2}} = \text{Trace } M_0 - \frac{2 \det M_0}{\text{Trace } M_0} + h.o.t.$$

$$= \text{Trace } M_0 - 2K_3(\beta-1) + h.o.t.$$

It follows that

$$\lambda^+ = K_3(1-\beta) + h.o.t. \tag{5D.8a}$$

and

$$\lambda^- = -\text{Trace } M_0 + K_3(\beta-1) + h.o.t.$$

$$= \frac{1}{m}K_2\epsilon(u_1+k)x_0^{-1+\epsilon/\lambda_1} - K_3\beta + h.o.t. \tag{5D.8b}$$

From (5D.7), it follows that $\lambda^+/\lambda^- \to 0$ and $\epsilon \to 0$. Eigenvalues corresponding to M_1 are $\hat{\mu}^{\pm} = x_0^{-\epsilon/\lambda_1}\lambda^{\pm}$. We therefore conclude that if $p \in H_2$, then $D\pi(p)$ has two real eigenvalues, μ^+ and μ^-, which satisfy $\mu^+/\mu^- \to 0$ as $\epsilon \to 0$.

We now wish to compute eigenvectors of $D\pi(p)$ which correspond to μ^+ and μ^-. These eigenvectors are perturbations of eigenvectors of M_0. Note that if

$$a^{\pm} = \frac{K_3,}{K_2\epsilon(u_1+k)x_0^{-1+\epsilon/\lambda_1} \pm m\lambda^{\pm}},$$

then $e^{\pm} = (a^{\pm} \quad 1)^{\top}$ are eigenvectors corresponding to $\lambda^{\pm}$. Now (5D.7) and (5D.8) imply that

$$a^+ = \frac{K_3}{K_2\epsilon(u_1+k)x_0^{-1+\epsilon/\lambda_1} + m(K_3-\beta) + h.o.t.} \to 0 \quad \text{as} \quad \epsilon \to 0,$$

and

$$a^- = \frac{1}{m\beta} + h.o.t. \quad (1/m\beta \quad 1)^\top$$

Therefore, $e^+ \to (0 \quad 1)^\top$ as $\epsilon \to 0$, and $\epsilon^- \to (1/m\beta \quad 1)^\top$ as $\epsilon \to 0$. We recall, from Section 3, that $m\beta \neq 0$.

We now assume that $p \in H_1$. It then follows from (5D.1) that $u_1 > -k + (\epsilon N_0/2)$ and

$$\frac{1}{2}\delta_z \left[\frac{m(u_1+k)}{2\delta_x}\right]^{\lambda_2/(\lambda_1-\epsilon)} \leq z_1 \leq 2\delta_z \left[\frac{2m(u_1+k)}{\delta_x}\right]^{\lambda_2/(\lambda_1-\epsilon)}.$$

Since, by (5D.2), $x_0 = \delta_x(z_1/\delta_z)^{\lambda_1/\lambda_2}$, there exist constants K_i, $i = 1, 2, \ldots$, such that

$$K_1(u_1+k)^{\lambda_1/(\lambda_1-\epsilon)} \leq x_0 \leq K_2(u_1+k)^{\lambda_1/(\lambda_1-\epsilon)}. \tag{5D.9}$$

Now (5D.1) and (5D.2) imply that, for ϵ sufficiently small,

$$x_0 \geq K_1(u_1+k)^{\lambda_1/(\lambda_1-\epsilon)} \geq K_3\left(\frac{N_0}{2}\epsilon\right)^{\lambda_1/(\lambda_1-\epsilon)} \geq K_4\epsilon$$

and

$$\begin{aligned} x_0 &\leq K_2(u_1+k)^{\lambda_1/(\lambda_1-\epsilon)} = K_2(u_0+k)\left(\frac{\delta_x}{x_0}\right)^{\epsilon/\lambda_1} \\ &\leq K_3(u_0+k) \leq K_3(H^0(0)+k) \\ &\leq K_3\epsilon. \end{aligned}$$

Moreover, (5D.9) implies that $(u_1+k)x_0^{-1}$ is bounded; say

$$0 \leq (u_1+k)x_0^{-1} \leq K_4.$$

These estimates imply that as $\epsilon \to 0$, $A \to 0$, $B \to (1/m)K_3$, $C \to 0$, and $D \to K_3$.

Therefore, the eigenvalues and corresponding eigenvalues of $D\pi(p)$ approach the eigenvalues and corresponding eigenvectors of the matrix

$$M_2 = \begin{bmatrix} 0 & (1/m)K_3 \\ 0 & K_3 \end{bmatrix}$$

as $\epsilon \to 0$. The eigenvalues of M_2 are, of course, 0 and K_3. Corresponding eigenvectors are $(1 \quad 0)^\top$ and $(1 \quad m)^\top$.

The preceding estimates demonstrate that (h2) and (h3) are satisfied if we chose μ small, let S^u be a sufficiently small sector around e^+, and let S^s be a sufficiently small sector around e^-.

Appendix

Each solution shown in Figure 1 is a solution of the following system due to Rinzel and Ermentrout [14]. It is based on the model of Morris and Lecar [12] for electrical activity in the barnacle muscle fiber.

$$\begin{aligned} u' &= y - .5(v + 5) - 2w(v + .7) - m_\infty(u)(u - 1) \\ w' &= 1.15(w_\infty(v) - w)\tau(u) \\ y' &= \epsilon(k - v) \end{aligned} \tag{A.1}$$

where

$$\begin{aligned} w_\infty(u) &= \frac{1}{2}\left[1 + \tanh\left(\frac{u - .1}{.145}\right)\right] \\ m_\infty(u) &= \frac{1}{2}\left[1 + \tanh\left(\frac{u + .01}{.15}\right)\right] \\ \tau(u) &= \cosh\left(\frac{u - .1}{.29}\right). \end{aligned}$$

For each solution in Figure 1, $\epsilon = .002$. For the solution shown in Figure 1A, $k = -.23$, for the solution shown in Figure 1B, $k = -.13$, and for the solution shown in Figure 1C, $k = -.1306$.

The following are the precise assumptions that were required in [17] for the existence of bursting solutions and continuous spiking. Further remarks concerning these assumptions are given in [17].

H1. The fixed points of (FS) consist of a smooth, S-shaped curve, $\mathcal{S}$ in phase space. That is, there exists $\lambda < \rho$ such that
   a. If $y < \lambda$ then (FS) has precisely one fixed point, which we denote by ℓ_y.
   b. If $y > \rho$, then (FS) has precisely one fixed point, which we denote by u_y.
   c. If $\lambda < y < \rho$, then (FS) has precisely three fixed points, which we denote by ℓ_y, m_y, and u_y.
   d. The fixed point at the "left knee," for $y = \lambda$, is denoted by K_λ, and the fixed point at the "right knee" is denoted by K_ρ.
   e. The union of all of these fixed points forms a smooth curve, which we denote by $\mathcal{S}$.

H2. Each of the fixed points ℓ_y is an attractor as a solution of (FS), and each of the fixed points m_y is a saddle. We denote the two trajectories in the unstable manifold of each m_y by $M_y^+(t)$ and $M_y^-(t)$.

H3. There exists $h \in (\lambda, \rho)$ such that $M_h^+(t)$ is homoclinic to M_h. If $y \in (\lambda, \rho)$, then $\lim_{t\to\infty} M_y^-(t) = \ell_y$. If $y \in (\lambda, h)$, then $\lim_{t\to\infty} M_y^+(t) = \ell_y$.

H4. There exists $\delta_0 > 0$ such that if $h < y < \rho + \delta_0$, then there exists an asymptotically stable periodic solution $p_y(t)$ of (FS). This periodic solution surrounds u_y, but neither ℓ_y nor m_y. The union of all of these periodic solutions form invariant, normally hyperbolic manifold $\mathcal{P}$, which terminates at $M_h^+(t)$ as $y \to h$.

Remark. In Figure 4, we illustrate the phase planes corresponding to (FS) for three different values of the parameter y. In each of these figures, $\lim_{t\to\infty} M_y^-(t) = \ell_y$. In Figure 4A, we assume that $\lambda < y < h$. In this case, $\lim_{t\to\infty} M_y^+(t) = \ell_y$. In Figure 4B, $y = h$, and $M_y^+(t)$ is the homoclinic orbit. Finally, in Figure 4C, $h < y < \rho$. In the case, $M_y^+(t)$ approaches the periodic orbit, $p_y(t)$, as $t \to \infty$.

We now need an assumption which allows us to conclude that for small ϵ, solutions of (2A.1) which pass close to the right knee must then pass close to the left knee must then pass close to the lower branch. In what follows, $w(\gamma_0)$ will be the omega limits set of the solution of (2A.1) which passes through γ_0.

H5. There exists a neighborhood $\mathcal{U}_\rho$ of K_ρ such that if $\gamma_0 = (v_0, y_0, w_0) \in \mathcal{U}_\rho$, then either $\omega(\gamma_0) = m_{y_0}, \omega(\gamma_0) = \ell_{y_0}, \omega(\gamma_0) = p_{y_0}$. There exists a neighborhood $\mathcal{U}_\lambda$ of K_λ such that if $\gamma_0 \in \mathcal{U}_\lambda$, then wither $\omega(\gamma_0) = m_{y_0}, \omega(\gamma_0) = \ell_{y_0}$, or $\omega(y_0) = u_{y_0}$.

The final assumptions are concerned with the slow dynamics.

H6. There exists $k_\rho < k_\lambda$ such that if $k_\rho < k < k_\lambda$ then $g(v, w, y, k) = 0$ if and only if $v = h(w, y, k)$ for some smooth function $h(w, y, k)$. Moreover, $g(v, w, y, k) < 0$ if and only if $u > h(w, y, k)$. If $M_k = \{(v, w, y) : v = h(w, y, k)\}$, then $M_k \cap \mathcal{S} = M_{y_k}$ for some $y_k \in (\lambda, \rho)$.

Let $M_k^+ = \{(v, w, y) : v > h(w, y, k)\}$ and $M_k^- = \{(v, w, y) : v < h(w, y, k)\}$.

H7. If $k_\rho < k < k_\lambda$, then $\{\ell_y : y < \rho\} \subset M_k^-$. Moreover, there exists a unique $k_h \in (k_\rho, k_\lambda)$ such that $y_{k_h} = h$. If $k_\rho \le k \le k_h$, then $\mathcal{P} \subset M_k^+$.

This last assumption implies that if $k \in (k_\rho, k_\lambda), \epsilon > 0$, and (v, w, y) lies near the lower branch, then $y' = \epsilon g(v, w, y, k) > 0$. If $k_\rho < k < k_h, \epsilon > 0$ and (v, w, y) lies near $\mathcal{P}$, then $y' < 0$. Note that if $k = k_h$ and $\epsilon > 0$, then the fixed point of (2A.1) is M_h. This is the homoclinic point of (2A.1) with $\epsilon = 0$.

H8. If $k_h < k < k_\lambda$, then $(\partial g/\partial k)(v, w, y, k) > 0$ in some neighborhood of the homoclinic orbit $M_y^+(t)$.

Remark. The last assumption (H8) is satisfied for the β-cell models discussed in the introduction. For these models, $\partial g/\partial k > 0$ everywhere.

Note that, after a suitable change of variables, the assumptions A1–A6 follow from H1–H8 if we impose the additional assumption that the center-stable and center-unstable manifolds to the middle branch intersect traversely at the homoclinic orbit $M_h^+(t)$.

A bursting solution is defined as periodic solution of (2A.1) whose trajectory in phase space alternates between passing close to the lower branch (the passive phase) and passing close to $\mathcal{P}$, the branch of periodic solutions (the active phase). We say that (2A.1) gives rise to continuous spiking if there exists a stable periodic of (2A.1) whose trajectory in phase space always lies near $\mathcal{P}$. In [17] we prove the following.

Theorem A.1. *(a)* Fix $k \in (k_p, k_h)$. *If ϵ is sufficiently small, then there exists a bursting solution of (2A.1).*

(b) There exists $k_0 > k_h$ with the following property: Fix $k \in (k_h, k_0)$. *If ϵ is sufficiently small, then (2A.1) gives rise to continuous spiking.*

Acknowledgement

Supported in part by the National Science Foundation under Grant No. DMS 9002349.

References

1. J. C. Alexander and D. Cai, On the dynamics of bursting systems, J. Math. Biol. **29**, 405 (1991).
2. P. M. Beigelman, B Ribalet, and I. Atwater, Electrical activity of mouse pancreatic β-cells II. Effects of glucose and arginine, J. Physiol. (Paris) **73** (1977), 201–217.
3. T. R. Chay, Chaos in a three-variable model of an excitable cell, Phys. D. 16 (1985), 233–242.
4. T. R. Chay and J. Keizer, Minimal model for membrane oscillations in the pancreatic beta-cell, Biophys. J. **42** (1983), 181–190.
5. T. R. Chay and J. Rinzel, Bursting, beating, and chaos in an excitable membrane model, Biophys. J. **47** (1985) 357–366.
6. B. Deng, Homoclinic bifurcations with nonhyperbolic equilibria, SIAM J. Math. Anal. **21** (1990), 693–720.
7. N. Fenichel, Persistence and smoothness of invariant manifolds for flows, Indiana Univ. Math. J. **21** (1971), 193–226.
8. J. Gukenheimer and P. Holmes, *Nonlinear Oscillations, Dynamical Systems, and Bifurcations of Vectors Fields,* Springer-Verlag, New York (1986).
9. A. L. Hodgkin and A. F. Huxley, A quantitative description of membrane current and its application to conduction and excitation in nerve, J. Physiol. (London) **117** (1952), 500–544.
10. H. P. Meissner, Electrical characteristics of the beta-cells in pancreatic islets. J. Physiol. (Paris) **72** (1976), 757–767.
11. J. Moser, *Stable and Random Motions in Dynamical Systems,* Princeton University Press, Princeton (1973).
12. C. Morris and H. Lecar, Voltage oscillations in the barnacle giant muscle fiber, Biophys. J. **35** (1981), 193–213.
13. J. Rinzel, *Bursting oscillations in an excitable membrane model,* in *Ordinary and Partial Differential Equations* (B. D. Sleeman and R. J. Jarvis, eds.), Springer-Verlag, New York (1985), 304–316.
14. J. Rinzel and G. B. Ermentrout, Analysis of neural excitability and oscillations, in *Methods in Neuronal Modeling, From Synapses to Networks,* (C. Koch and I. Seger, eds.), MIT Press, Cambridge, MA (1989), 135–169.
15. A. M. Scott, I. Atwater, and E. Rojas, A method for the simultaneous measurement of insulin release and beta-cell membrane potential in single mouse islet of Langerhans, Diabetologia **21** (1981), 470–475.
16. A. Sherman, J. Rinzel, and J. Keizer, Emergence of organized bursting in clusters of pancreatic β-cells by channel sharing, Biophys. J. **54** (1988), 411–425.
17. D. Terman, Chaotic spikes arising from a model for bursting in excitable membranes, SIAM J. Appl. Math. **51** (1991), 1418–1450.
18. S. Wiggins, *Global Birfurcations and Chaos: Analytic Methods,* Springer-Verlag, New York, Heidelberg, Berlin (1988).